Reduced Hydrogen Sulfide Bioavailability Contributes to Cardiometabolic Heart Failure with Preserved Ejection Fraction

Jake E. Doiron, Ph.D.[2]*, Mahmoud H. Elbatreek, Ph.D.[1,10]*, Huijing Xia Ph.D.[2], Xiaoman Yu, M.S.[1], W.H. Wilson Tang M.D.[3,4], Kyle B. LaPenna Ph.D.[2], Thomas E. Sharp III Ph.D[5], , Traci T. Goodchild Ph.D.[1], Ming Xian, Ph.D.[6], Shi Xu, Ph.D.[6], Heather Quiriarte, M.S.[7], Timothy D. Allerton Ph.D.[7], Alexia Zagouras, M.D. M.S.[3], Jennifer Wilcox, B.S.[3], Sanjiv J. Shah, M.D.[8], Josef Pfeilschifter[9], Karl-Friedrich Beck[9], Zhen Li, Ph.D.[1], David J. Lefer Ph.D.[1#]

[1] Department of Cardiac Surgery, Smidt Heart Institute, Cedars-Sinai Medical Center, Los Angeles, CA
[2]Department of Pharmacology and Cardiovascular Center, Louisiana State University Health Sciences Center, New Orleans, LA
[3]Department of Cardiovascular Medicine, Heart, Vascular and Thoracic Institute, Cleveland Clinic, Cleveland, OH
[4]Center of Microbiome and Human Health, Department of Cardiovascular and Metabolic Sciences, Lerner Research Institute, Cleveland Clinic, Cleveland, Cleveland, OH
[5]Molecular Pharmacology and Physiology, University of South Florida, Tampa, FL
[6]Department of Chemistry, Brown University, Providence, RI
[7] Vascular Metabolism Laboratory, Pennington Biomedical Research Center, Baton Rouge, LA
[8] Northwestern University Medicine, Feinberg School of Medicine, Chicago, IL
[9]Institute of Pharmacology and Toxicology, Goethe University, Frankfurt am Main, Germany
[10]Department of Pharmacology and Toxicology, Faculty of Pharmacy, Zagazig University, Zagazig, Egypt

*: J.D. and M.E. contributed equally

Running Title: Hydrogen sulfide in HFpEF

Word Count: 9126

[#] **Address for correspondence:**

David J. Lefer, Ph.D., Department of Cardiac Surgery, Smidt Heart Institute, Cedars-Sinai Medical Center, Los Angeles, CA 90048. Phone: +1 (310) 423-7483, Email: David.Lefer@cshs.org

Author/funding disclosures:

These studies were supported by grants from the National Institutes of Health HL146098, HL146514, and HL151398 to D.J.L., HL159428 to T.T.G., AA029984 to T.E.S. and by an American Heart Association Postdoctoral fellowship to Z.L. (20POST35200075). P20GM135002 and U54GM104940 to T.D.A. J.E.D. is the recipient of a training fellowship from the NIH National CCTS awarded to the University of Alabama at Birmingham as part of a TL1 Training Grant (TL1TR003106).

D.J.L. serves as an unpaid consultant for Sulfagenix, Inc. Sulfagenix is currently developing H_2S-based therapeutics for a number of clinical indications including cardiovascular diseases. The other authors declare no conflicts of interest.

Tweet: Hydrogen sulfide (H_2S) deficiency is linked to heart failure with preserved ejection fraction (HFpEF) in humans and animal models. Reduced production by CSE and increased metabolism by SQR impair H_2S bioavailability. Targeting H_2S may offer new therapeutic strategies for HFpEF. **#LeferLab #HeartFailure #H_2SResearch**.

ABSTRACT

Background: Heart failure with preserved ejection fraction (HFpEF) is a significant public health concern with limited treatment options. Dysregulated nitric oxide-mediated signaling has been implicated in HFpEF pathophysiology, however, little is known about the role of endogenous hydrogen sulfide (H_2S).

Objectives: This study evaluated H_2S bioavailability in patients and two animal models of cardiometabolic HFpEF and assessed the impact of H_2S on HFpEF severity through alterations in endogenous H_2S production and pharmacological supplementation.

Methods: HFpEF patients and two rodent models of HFpEF ("two-hit" L-NAME + HFD mouse and ZSF1 obese rat) were evaluated for H_2S bioavailability. Two cohorts of two-hit mice were investigated for changes in HFpEF pathophysiology: (1) endothelial cell cystathionine-γ-lyase (EC-CSE) knockout; (2) H_2S donor, JK-1, supplementation.

Results: H_2S levels were significantly reduced (i.e., 81%) in human HFpEF patients and in both preclinical HFpEF models. This depletion was associated with reduced CSE expression and activity, and increased SQR expression. Genetic knockout of H_2S -generating enzyme, CSE, worsened HFpEF characteristics, including elevated E/e' ratio and LVEDP, impaired aortic vasorelaxation and increased mortality. Pharmacologic H_2S supplementation restored H_2S bioavailability, improved diastolic function and attenuated cardiac fibrosis corroborating an improved HFpEF phenotype.

Conclusions: H_2S deficiency is evident in HFpEF patients and conserved across multiple HFpEF models. Increasing H_2S bioavailability improved cardiovascular function, while knockout of endogenous H_2S production exacerbated HFpEF pathology and mortality. These results suggest H_2S dysregulation contributes to HFpEF and increasing H_2S bioavailability may represent a novel therapeutic strategy for HFpEF.

KEY WORDS

H_2S, HFpEF, ZSF1 Obese, CSE, SQR, H_2S donor.

Highlights

- H_2S deficiency is evident in both human HFpEF patients and two clinically relevant models.
- Reduced H_2S production by CSE and increased metabolism by SQR impair H_2S bioavailability in HFpEF.
- Pharmacological H_2S supplementation improves diastolic function and reduces cardiac fibrosis in HFpEF models.
- Targeting H_2S dysregulation presents a novel therapeutic strategy for managing HFpEF.

ABBREVIATIONS AND ACRONYMS

CSE	cystathionine-γ-lyase
HFpEF	heart failure with preserved ejection fraction
HFrEF	heart failure with reduced ejection fraction
L-NAME	N(ω)-nitro-L-arginine methyl ester
LV	left ventricle
SNP	sodium nitroprusside
SQR	sulfide quinone oxidoreductase
WKY	Wistar Kyoto
ZSF1	Zucker fatty and spontaneously hypertensive

INTRODUCTION

Heart failure with preserved ejection (HFpEF) fraction is a significant public health concern. The increasing prevalence of HFpEF risk factors has resulted in HFpEF diagnoses accounting for 50% of all new heart failure diagnoses, while the subsequent pathophysiology leaves HFpEF patients subject to a 23% 30-day hospital readmission rate and 50-75% 5-year mortality rate[1-4]. As our knowledge of HFpEF progresses, understanding not only the cardiovascular, but also systemic drivers of the condition are crucial. The influence of the physiologic gaseous mediator, nitric oxide (NO), has been extensively investigated in both preclinical and clinical studies[5,6]. While the precise role of NO signaling and nitrosative stress in HFpEF is still being elucidated, little is known about other endogenous gaseous molecules, particularly hydrogen sulfide (H_2S).

Since its discovery as an endogenously-produced and biologically essential molecule in 1996, H_2S has garnered significant attention for its role in maintaining whole-body and cardiovascular homeostasis[7]. H_2S biosynthesis is regulated through three key enzymes, cystathionine-β-synthase (CBS), cystathionine-γ-lyase (CSE) and 3-mercaptopyruvate sulfurtransferase (3-MST)[8-10]. The major catabolic pathway of H_2S occurs in the mitochondria under the control of sulfide quinone oxidoreductase (SQR)[11]. Perturbations in H_2S bioavailability have been implicated in numerous cardiovascular pathologies, including atherosclerosis, hypertension, myocardial infarction, and heart failure with reduced ejection fraction (HFrEF)[12-15]. Investigation of H_2S in these pathologies has revealed that H_2S exerts potent antioxidant, anti-inflammatory, metabolic regulatory, and mitochondrial preservation actions[16-20]. Additionally, H_2S has significant interplay with NO, whereby H_2S augments cardioprotective endothelial nitric oxide synthase (eNOS) signaling[21]. Considering that HFpEF is characterized by derangements in metabolism, inflammation, oxidative stress and NO signaling, H_2S is a promising prospect for further investigation in HFpEF.

Of the HFpEF phenotypes, cardiometabolic HFpEF is of increasing importance given its reputation as the most prevalent HFpEF phenotype in a syndrome growing in incidence and

diagnoses[1,22]. Cardiometabolic HFpEF now comprises an estimated 33% of the HFpEF patient population and is most frequently comorbid with obesity, diabetes, hypertension, chronic low-grade inflammation, and hepatic injury[23,24]. Interestingly, H_2S deficiency has been associated with these independent comorbidities and replenishment of H_2S has been shown to improve the respective pathologies[9,17,25-29]. In the present study, we sought to evaluate alterations in H_2S bioavailability and the role of H_2S in HFpEF using multiple clinically relevant models of cardiometabolic HFpEF. We also investigated the potential beneficial actions of H_2S therapy in the form of H_2S donors in the setting of HFpEF.

METHODS

Human Plasma Samples

Plasma samples were collected from either ambulatory patients with HFpEF prospectively enrolled in an outpatient clinic (with signs and symptoms or heart failure and echocardiogram showing left ventricular ejection fraction ≥50%) or age- and sex-matched healthy participants recruited from the community without existing cardiovascular diseases (confirmed by echocardiography, pulmonary function testing, and cardiac biomarkers) under protocols approved by the Institutional Review Board (IRB# 06-805 and #10-727, respectively) at the Cleveland Clinic. All participants provided written informed consent to participate. Baseline characteristics of all participants are shown in ***Table 1***.

Measurement of Plasma hs-CRP

The levels of hsCRP (#EA101010, ORIGENE, Rockville, MD) in plasma samples from control of HFpEF patients were measured with commercially available ELISA assay kits according to manufacturer's instructions.

Experimental Animal Models of HFpEF

"Two-hit" Mouse Model of HFpEF: Male C57BL/6N (Charles Rivers Laboratories, Wilmington, MA, USA) mice were purchased at 8 weeks of age and allowed to acclimatize for one week prior to study enrollment. Starting at 9 weeks of age, male C57BL/6N were treated with either L-N^G-nitro arginine methyl ester (L-NAME, Enzo Biochem, Farmingdale, NY, USA) in the drinking water (0.5 gram/L) and 60% kcal high fat diet (HFD, D12492, Research Diets, New Brunswick, NJ, USA) to induce HFpEF (n = 7-10 per group), or normal drinking water and normal diet (Teklad 2019s, Inotiv, Chicago, IL, USA) (n = 7-10 per group). C57BL/6N mice were maintained on HFpEF treatment for 0, 5 or 10 weeks prior to physiological characterization. Similarly, male endothelial cell-cystathionine-γ-lyase (EC-CSE) knockout (KO), EC-CSE transgenic (Tg) and age-matched littermate controls were generated as described previously.[30] At 9 weeks of age, animals were enrolled to L-NAME and HFD treatment for 18 weeks. Lastly, for the H_2S treatment intervention with H_2S donor, JK-1, male C57BL/6N were enrolled

at 9 weeks of age and began L-NAME and HFD treatment. At 5 weeks of L-NAME and HFD, mice were further randomized to either receive JK-1 (100µg/kg, b.i.d, i.p.) or vehicle (saline, b.i.d, i.p.). Group sizes of n = 7-10 were determined using a power and sample analysis with the significance level at 5% and power at 80%.

ZSF1 Obese Rat Model of Cardiometabolic HFpEF: Wistar Kyoto and ZSF1 obese rats (Charles River Laboratories, Wilmington, MA, USA) were purchased at 8 weeks of age to acclimatize for at least 2 weeks prior to study enrollment. Group sizes of n = 6 - 8 were determined using a power and sample analysis with the significance level at 5% and power at 80%. Mice and rats were housed at LSUHSC and CSMC in a temperature controlled and 12-hour light/dark cycle. All studies were LSUHSC and CSMC IACUC (Institutional Animal Care and Use Committee) approved and received care in LSUHSC animal care according to AALAC guidelines.

Non-Fasting Blood Glucose

A blood drop from the rat tail was used to measure non-fasting blood glucose with an Accu-Check Guide glucometer (Roche, Indianapolis, IN, USA).

Hydrogen Sulfide Donor

JK-1 was synthesized by Dr. Ming Xian et al. as previously reported[31]. The dosage of JK-1 (100 µg/kg, b.i.d) was determined based on our previous studies of JK-1 in murine models of CV disease [32-34].

Exercise Capacity Testing

Treadmill exercise capacity of either mice or rats was performed using an IITC Life Science 800 Series rodent specific treadmill (Woodland Hills, CA). For mice, animals were first allowed to acclimate to the treadmill environment for a period of 5 minutes. Following acclimation, the mice were subjected to a warm-up protocol on a flat plane starting at 1 meter per minute (m/min) that began increasing by 1.1m/min until a final speed of 12m/min was achieved after 10 minutes and then subsequently maintained for an additional 5 minutes. After the 15-minute warm-up, the ramp was increased to a 30°

incline and the exercise capacity of the mice were recorded during an experimental protocol starting at 12m/min that increased by 2m/min until a final speed of 18m/min was achieved and maintained until the mouse reached a state of exhaustion.

Rats were allowed to acclimate to the treadmill environment for a period of 5 minutes. After acclimation, a warm-up protocol on a flat plane was initiated consisting of a starting speed of 6m/min with a gradual increase of 1.5m/min until a final speed of 12m/min was achieved and maintained for an additional minute. After the 5-minute warm-up, the animal's exercise capacity was recorded during an experimental run on a flat plane at a consistent speed of 12m/min until the animal reached a state of exhaustion. Exhaustion was determined as an animal refusing to run for greater than 5 seconds or an inability of the animal to reach the front of the treadmill for 20 seconds. Data are represented as both exercise distance and work (kg*m) utilizing the animal's body weight immediately prior to exercise testing.

Transthoracic Echocardiography

Echocardiography was performed utilizing a Vevo-2100 ultrasound system (Visual Sonics, Toronto, Canada) for mice and rats. Animals were shaved 18 hours prior to experimentation. Animals were induced at 3% isoflurane and maintained at 1-3% isoflurane for echocardiographic evaluation. For mice, recordings pertaining to diastolic function occurred at a target heart rate of >400 beats per minute (bpm) and >450 bpm for systolic measures. For rats, a target heart rate of >300 bpm was used for systolic and diastolic measures. Left ventricular ejection fraction (LVEF) was quantified using an M-mode image across the parasternal short-axis view. Early filling velocity (E), atrial filling velocity (A), and early diastolic tissue velocity (E') were measured in the four-chamber apical view. Data are represented as averages of three consecutive measurements for each parameter.

Systemic and Left Ventricular Hemodynamic Measurements

Left ventricular end-diastolic and systemic pressures were measured as previously described.[32] In brief, at the study endpoint, animals were anesthetized at 3% isoflurane until unresponsive to stimuli. The right common carotid artery was further surgically isolated and exposed. Once exposed, the isoflurane was

reduced to 1% while a 1.4Fr (for mice) or 1.6Fr (for rats) high-fidelity pressure catheter (Transonic, NY, USA) was inserted and measurements of systemic blood pressures were recorded. The catheter was then advanced into the left ventricular lumen for measurement of left ventricular end-diastolic pressure (LVEDP).

Ex Vivo Aortic Ring Vascular Reactivity

Thoracic aortas of mice or rats were removed for vascular reactivity testing at sacrifice as previously described.[35] In brief, thoracic aortic rings were first equilibrated in Krebs-Henseleit solution and provided a tension of 0.5 grams for 60 minutes to reach equilibration. The rings were then pretreated with phenylephrine for maximal constriction and then followed with challenges of titrated acetylcholine (10^{-9} to 10^{-5} M) and subsequently sodium nitroprusside (10^{-9} to 10^{-5} M) and measured relaxation as compared to phenylephrine maximal contraction. Data are reported as percent relaxation from the maximum contraction to phenylephrine.

Hydrogen Sulfide and Sulfane Sulfur Measurements

Hydrogen sulfide and sulfane sulfur were measured in plasma and tissue samples utilizing a gas chromatography-sulfur chemiluminescence system (Agilent Technologies, Santa Clara, CA, USA) as previously described[18].

Real-Time PCR

Total RNA from tissues was extracted with TRIzol (Life Technologies Corporation, USA). First strand cDNAs were obtained with iScrip Reverse Transcription Supermix (Bio-Rad, USA). Quantitative real-time PCR was performed with SYBR Green qPCR Master Mix (Selleck Chemicals, USA) on CFX Duet (Bio-Rad, USA). $2^{-\Delta\Delta Ct}$ method was utilized to calculate relative expression to 18s/Tubb5. Primer sequences used in the current study are listed in **Supplemental Table 1**.

Western blot

Immunoblot analysis was performed on samples lysed in RIPA lysis buffer (Medchemexpress, USA) with the addition of Phosphatase Inhibitor (Selleck Chemicals, USA) and Protease Inhibitor Cocktail

Mini-Tablet (Medchemexpress, USA) using standard procedures. The protein concentration was determined with BCA Protein Assay Kits (Thermo, USA). Total protein was separated with SDS-PAGE and transferred onto PVDF membranes (Gen Hunter Corporation, USA). Western blot analysis was performed using commercially available antibodies: CSE Polyclonal Antibody (1:2,000, PA5-29725; Thermo, USA), Anti-SQRDL Antibody (1:1,000, 144-09256-20; Ray Biotech, USA). Total protein staining used as loading control was obtained utilizing No-Stain™ Protein Labeling Reagent (Invitrogen, USA). Where mentioned, proteins were assessed using ImageJ software to analyze the optical density of western blots normalized to loading control.

Enzyme Activity Assay

Enzyme reactions to determine the production of H_2S from CSE were performed as described previously[36] with slight modification. Briefly, tissues were homogenized in buffer containing 100 mM potassium phosphate, pH 7.4. For enzyme reactions, 0.172 mL of homogenate was incubated with 0.028 mL of substrate mix (10 mM L-cysteine, 2 mM pyridoxal 5′ -phosphate) in a sealed vial at 37°C for 30 minutes. After adding 0.400 ml of 1 M sodium citrate buffer (pH 6.0), the mixtures were incubated at 37°C for 15 min with shaking on a rotary shaker to facilitate a release of H_2S gas from the aqueous phase. After shaking, 0.1 mL of head-space gas was applied to a gas chromatograph as described above. For both reactions, the H_2S concentration of each sample was calculated against a calibration curve of Na_2S.

Histology and Fibrosis

Cardiac, renal cortex, and hepatic samples were collected and preserved in a 10% zinc formalin buffered solution (CUNZF-5-G, Azer Scientific, Morgantown, PA, USA) for 48 hours, after which they were transferred to a storage solution of 0.01% sodium azide in PBS. The samples were then embedded in paraffin and sectioned into 5 μm thick cross-sections. These sections were stained using either hematoxylin and eosin or picrosirius red with fast green counterstaining. Images were processed with QuPath software and analyzed using ImageJ to quantify cardiac interstitial and perivascular fibrosis, as well as renal interstitial, perivascular, and periglomerular fibrosis, along with hepatic lipid content. For

each animal, a minimum of 10 areas, vessels, or glomeruli within the tissue section were analyzed. Initially, images were converted to 8-bit grayscale with an RGB stack, and the threshold was adjusted to quantify lipid droplet features and the percentage of fibrosis.

Statistical Analysis

Data are presented using both mean ± SEM and box plots (median, minimum, and maximum). All statistical analysis were performed in a blinded manner using the Prism 6 and Prism 10 software (GraphPad, San Diego, California). Differences in data among 2 groups were compared using an unpaired student t-test. For comparisons amongst multiple, separate groups of animals enrolled within the same experimental study, multiple unpaired student *t* tests were utilized. For data involving animal cohorts that were continuously monitored and evaluated according to factors such as timepoints or concentrations, 2-way ANOVA analysis followed by a Bonferroni multiple comparison test was utilized. Survival data was acquired using a Kaplan-Meier survival curve analysis through Prism 6. A p value of <0.05 was considered statistically significant. The presented data may have different numbers of animals per group as only a subset of the mice or rats from each group were used for certain experiments. Additionally, exclusion of animals was carried out due to complications such as procedural failure in invasive hemodynamics measurement, limited amount of sample collected (i.e., plasma volume), and lack of participation in treadmill running. Prior to conducting statistical analysis, an outlier test was performed using a Grubbs test ($\alpha = 0.05$) through GraphPad to identify and remove any outliers in the data set.

RESULTS

H_2S is Depleted in Human HFpEF

To investigate the role of H_2S in HFpEF, we collected plasma samples from patients with confirmed HFpEF (n=46) and a control group without HFpEF (n=45) (***Figure 1A***). The characteristics of the patient population are detailed in Table 1. Our analysis revealed an 81% reduction in circulating H_2S levels in the HFpEF patients, accompanied by significant decreases in sulfane sulfur levels (***Figure 1B and 1C***). Additionally, we observed elevated levels of the inflammatory marker hs-CRP in the HFpEF group (***Figure 1D***).

H_2S is Reduced in Mouse Two-Hit HFpEF Model Due to Decreased Production by CSE

We next employed a well-established "two-hit" cardiometabolic HFpEF mouse model (L-NAME + HFD)[5], to assess H_2S bioavailability and HFpEF phenotype after 0, 5, or 10 weeks of treatment as outlined in ***Figure 2A***. We first characterized the HFpEF phenotype in this model. Mice with HFpEF exhibited increased body weights and elevated systolic and diastolic blood pressures (***Figure 2B-2D***). While left ventricular ejection fraction (LVEF) remained within a preserved range, the E/e' ratio increased throughout the treatment (***Figure 2E and 2F***). Correspondingly, left ventricular catheterization revealed elevated left ventricular end-diastolic pressure (LVEDP), indicating increased myocardial stiffness and reduced compliance (***Figure 2G***). Additionally, HFpEF mice displayed substantially diminished exercise capacity, as evidenced by reduced exercise distance (***Figure 2H***). Endothelial dysfunction was also noted, with impaired aortic vasoreactivity to acetylcholine, though responsiveness to sodium nitroprusside remained unchanged (***Figure 2I and 2J***).

At baseline, no differences were observed in circulating H_2S; however, exposure to L-NAME and HFD resulted in a progressive decline in both circulating H_2S and sulfane sulfur levels (***Figure 3A and 3B***). Similarly, cardiac H_2S and sulfane sulfur levels decreased progressively throughout the two-hit regimen (***Figure 3C and 3D)***. To investigate the underlying causes of H_2S reduction, we examined the primary vascular H_2S-producing enzyme, CSE, and the main H_2S-metabolizing enzyme, SQR[8,9]. In the hearts of

HFpEF mice, both gene and protein expression, as well as enzyme activity of CSE, were significantly reduced (***Figure 3E-3G***), while SQR expression remained comparable to that in control hearts (***Figure 3H and 3I***)

Given the systemic nature of HFpEF, we also assessed H_2S bioavailability in hepatic and renal tissues, which are key organs for H_2S production and metabolism. We observed significant reductions in hepatic H_2S, along with decreased CSE gene and protein expression at the 10-week endpoint, although CSE activity did not differ from controls (***Supplemental Figure 1A-1D***). Notably, hepatic SQR gene expression was elevated in HFpEF, while protein levels remained unchanged (***Supplemental Figure 1E and 1F***). In the kidneys, no significant differences in H_2S levels were noted between control and HFpEF models at the 10-week endpoint (***Supplemental Figure 2A)***. However, renal CSE gene and protein expression, as well as enzyme activity, were significantly reduced in HFpEF, while SQR expression levels were similar to controls (***Supplemental Figure 2B-2F***).

These changes in systemic H_2S bioavailability correlate with the worsening HFpEF phenotype. Our data demonstrate that the "two-hit" L-NAME + HFD murine model develops a progressively obese and hypertensive phenotype, accompanied by a systemic depletion of bioavailable H_2S, primarily due to dysfunctional CSE in multiple organs.

Genetic Deficiency of CSE Exacerbates HFpEF Phenotype

To further explore the potential causal relationship between CSE dysfunction and global H_2S reduction, as well as to assess the impact of decreased H_2S bioavailability on HFpEF severity, we investigated mice with a knockout of endothelial cell cystathionine-γ-lyase (EC-CSE). EC-CSE knockout (KO) mice and their wild-type littermates underwent the same L-NAME and HFD HFpEF protocol (***Figure 4A***). Although circulating H_2S levels remained unchanged in the EC-CSE KO mice, sulfane sulfur levels were significantly reduced (***Figure 4B and 4C***). Cardiac H_2S levels were notably diminished in the knockout group, while cardiac sulfane sulfur levels were similar between the two groups (***Figure 4D and 4E***). The relative levels of cardiovascular H_2S and sulfane sulfur in EC-CSE KO mice align with previously

reported findings, indicating that despite the absence of plasma H_2S reductions, knockout mice still experience significant cardiovascular dysfunction[37].

All mice exhibited preserved ejection fractions (***Figure 4F***), but the lack of endothelial CSE resulted in elevated E/e' ratios and LVEDP (***Figure 4G and 4H***). We did not observe any significant differences in exercise capacity, which contrasts with earlier studies involving EC-CSE KO mice (***Figure 4I***)[30,37]. To assess vascular dysfunction in the context of CSE deficiency and HFpEF, we evaluated isolated thoracic aortic rings exposed to increasing concentrations of acetylcholine. Knockout animals demonstrated reduced vasorelaxation in response to acetylcholine (***Figure 4J***). Importantly, these changes in vascular reactivity were independent of altered responses to sodium nitroprusside, suggesting that the observed effects stem from compromised endothelial function (***Figure 4K***). Notably, the genetic deficiency of EC-CSE was associated with increased mortality in our study, underscoring the critical role of H_2S homeostasis in HFpEF (***Figure 4L***).

Exogenous H_2S Administration Ameliorates Systemic HFpEF Dysfunction

From a translational perspective, we aimed to determine whether the H_2S deficiency observed in HFpEF mice could be addressed with an exogenous pharmacological source of H_2S. We enrolled a cohort of wild-type mice in the two-hit HFpEF protocol, where they received L-NAME and HFD for 5 weeks to induce HFpEF. After this period, mice were randomized to receive either a saline vehicle or the H_2S donor JK-1 for an additional 5 weeks until the study endpoint (***Figure 5A***). Mice treated with JK-1 exhibited significantly higher levels of circulating and cardiac sulfane sulfur, without notable increases in free H_2S (***Figure 5B-5E***). The short half-life of free H_2S, combined with the pharmacokinetic profile of JK-1, likely accounts for the lack of elevated H_2S levels; however, the increased sulfane sulfur indicates a significant enhancement in the physiological sulfur pool.

Exogenous H_2S supplementation did not affect systolic blood pressure but resulted in a significant reduction in diastolic blood pressure (***Figure 5F and 5G***). Moreover, animals treated with JK-1 showed

statistically significant decreases in both E/e' and LVEDP (***Figure 5H and 5I***). JK-1 treatment also significantly improved exercise capacity (***Figure 5J***). These results are noteworthy, as HFpEF is characterized by severe exercise intolerance, and our findings suggest that H_2S therapy enhanced exercise capacity even in the presence of an eNOS inhibitor, indicating that the benefits of H_2S in HFpEF may not rely solely on NO signaling[38].

H_2S has been shown to exert anti-fibrotic effects in models of myocardial infarction and HFrEF, prompting us to evaluate myocardial interstitial and perivascular fibrosis[32]. We observed significant reductions in both perivascular and interstitial fibrosis following JK-1 treatment (***Figure 5K and 5L***). Additionally, our initial characterization of the L-NAME + HFD two-hit model indicated compromised hepatic H_2S bioavailability. Hepatic H_2S is crucial for liver health, and diminished hepatic H_2S signaling has been linked to the development of non-alcoholic fatty liver disease (NAFLD), a condition recently proposed as a predictor of HFpEF diagnosis[25,39]. Notably, we found substantial reductions in hepatic lipid content in HFpEF mice treated with JK-1 for 5 weeks, further supporting the potential benefits of H_2S in this systemic condition (***Figures 5M***).

Altered H_2S Production by CSE and Metabolism by SQR Underpins Cardiometabolic HFpEF in ZSF1 Obese Rats

To further validate our earlier findings in humans and mice, we investigated H_2S bioavailability in a clinically relevant model of cardiometabolic HFpEF using ZSF1 obese (Ob) rats[40,41]. For this study, we enrolled ZSF1 Ob rats and normotensive, non-obese, non-diabetic control Wistar Kyoto (WKY) rats. We comprehensively characterized the cardiometabolic HFpEF phenotype in ZSF1 Ob rats, monitoring HFpEF progression from week 10 to week 26 of age (***Figure 6A***). Key cardiometabolic parameters, including body weight, blood glucose levels, systolic and diastolic blood pressures, E/e' ratio, and LVEDP, were significantly elevated in ZSF1 Ob rats compared to WKY controls, while LVEF was preserved, and exercise capacity was impaired (***Figure 6B-6I***). Notably, circulating H_2S and sulfane

sulfur levels were dramatically reduced as early as 10 weeks of age in the ZSF1 obese rats (***Figure 6J and 6K***). The reduction in circulating H_2S and sulfane sulfur in the ZSF1 obese rat is very similar to that observed in HFpEF patients (i.e., ~80-90%).

We also examined CSE and SQR expression in the heart, liver, and kidneys. While cardiac CSE gene expression did not differ between WKY and ZSF1 Ob rats, CSE protein levels were lower in the ZSF1 Ob group. Conversely, both SQR gene and protein expressions were elevated in these rats (***Figure 7A-7D***). In the liver, we observed significant reductions in both CSE gene and protein expression, with unchanged SQR gene expression but increased SQR protein levels in ZSF1 Ob rats (***Figure 7E-7H***). In the kidneys, CSE expression was increased, while SQR expression was decreased at both the gene and protein levels (***Figure 7I-7L***).

In the heart, interstitial and perivascular fibrosis were pronounced in ZSF1 Ob rats **(*Figure 8A and Supplemental Figure 3A***), and H_2S levels were reduced despite unchanged CSE enzyme activity (***Figure 8B and 8C***). In the liver, lipid content was markedly increased, accompanied by substantial reductions in both H_2S levels and CSE enzyme activity (***Figure 8D-8F***). The kidneys of ZSF1 Ob rats also exhibited significant perivascular, interstitial, and periglomerular fibrosis (***Figure 8G and Supplemental Figure 3B and 3C***), with reduced H_2S levels and CSE enzyme activity observed by week 26 (***Figure 8H and 8I***).

These findings further confirm the presence of global H_2S deficiency as a consistent feature across multiple HFpEF models.

DISCUSSION

In this study, we identified systemic reductions in H_2S as a potential contributor to the development of cardiometabolic HFpEF, evident in both human patients and two distinct preclinical models. Our data indicate that H_2S deficiency and HFpEF pathology was remediated following the administration of pharmacological agents that release H_2S. Our data show that H_2S deficiency in HFpEF emerges from reduced tissue CSE expression and activity, and increased tissue SQR expression.

Our findings reveal a remarkable ~80% reduction in circulating H_2S levels in plasma from HFpEF patients compared to non-failing controls. This dramatic decrease in H_2S bioavailability far exceeds the ~40-50% reduction reported in HFrEF cases[14], suggesting that H_2S deficiency may play an equally or more significant role in HFpEF pathophysiology. Correspondingly, our preclinical models demonstrated a 60% reduction in circulating H_2S in the two-hit mouse model and up to 90% in ZSF1 Ob rats. Notably, the ZSF1 Ob rat exhibits a more pronounced H_2S deficiency that closely mirrors the clinical observations in HFpEF patients, thereby establishing it as a more relevant translational model.

We further examined H_2S levels across various organs including the heart, liver, and kidney given the systemic nature of HFpEF. In the two-hit mouse model, we observed a progressive decline in H_2S levels corresponding to the duration of L-NAME and HFD treatment. In ZSF1 Ob rats, circulating H_2S levels were already diminished by 10 weeks of age, with reductions noted in all examined peripheral organs as the animals aged. These findings suggest that early reductions in circulating H_2S could serve as pivotal biomarkers for the onset of HFpEF.

Utilizing the two-hit mouse model, we confirmed the presence of pronounced diastolic dysfunction, exercise intolerance, and metabolic dysregulation, consistent with previous studies[5,35]. The observed H_2S deficiency was primarily attributable to decreased expression and activity of CSE in peripheral organs. While CSE is constitutively expressed in the liver, kidneys, vasculature, and heart, vascular endothelial cells as well as the liver and kidney[9,11,44] are believed to be the primary regulators

of circulating H_2S levels. Our experiments with endothelial CSE knockout mice revealed that the depletion of this physiological sulfur pool exacerbated cardiac and vascular dysfunction. Conversely, exogenous H_2S therapy with the H_2S donor, JK-1, resulted in cardiovascular beneficial effects and marked improvements in exercise capacity. Indeed, previous studies show that CSE-derived H_2S has multiple cardiovascular benefits including vasorelaxation[45-47], angiogenesis regulation[46,48,49], atheroprotection[50-53] and reduced myocardial remodeling[54-57].

The interplay between H_2S and NO signaling has been well documented in cardiovascular disease models. NO can enhance H_2S production by increasing CSE transcription, highlighting the interdependence of these two signaling pathways[8]. Furthermore, H_2S-mediated effects, including vasorelaxation and cytoprotection, necessitate functional eNOS activity[8,21,46]. Conversely, H_2S donation can enhance eNOS-mediated NO production through mechanisms such as serine phosphorylation and S-sulfhydration[21,58]. The two-hit L-NAME and HFD model suggests that iNOS-driven over-nitrosylation of proteins is a key factor in HFpEF pathogenesis[5]. However, excessive protein S-nitrosylation alone does not fully account for HFpEF, as sodium nitrite administration does not worsen the condition and partially improves outcomes in the two-hit HFpEF model[35]. Finally, and NO pathway modulators show neutral effects in clinical trials[59-61]. This suggests that multiple factors contribute to an imbalance in NO signaling, leading to detrimental nitrosylation of specific proteins. Additionally, S-sulfhydration and S-nitrosylation may compete for the same cysteine residues, with H_2S deficiency potentially exacerbating pathological S-nitrosylation[58]. H_2S also acts as an antioxidant, enhancing the bioavailable NO pool by reducing peroxynitrite formation. Therefore, understanding both NO and H_2S signaling is crucial in the progression of HFpEF, highlighting their interconnected roles in cardiovascular diseases. Given this intricate crosstalk, the dysregulation of H_2S in our two-hit HFpEF model raises critical questions about its implications for NO signaling.

Our observations in ZSF1 Ob rats further corroborate the results from the two-hit model, as this model is characterized by a comprehensive phenotype that includes hypertension, obesity, diabetes, diastolic dysfunction, exercise intolerance, non-alcoholic fatty liver disease (NAFLD), and renal impairment[41,62,63]. Notably, the ZSF1 Ob rats exhibited even greater reductions in circulating, hepatic, and renal H_2S levels, potentially elucidating the observed hepatic and renal pathologies in this model[62,63]. While both models share reductions in CSE expression and activity, ZSF1 Ob rats demonstrated increased SQR expression. The later enzyme catalyzes the first irreversible step in the metabolism of H_2S, and thus plays a pivotal role in the regulation of H_2S-mediated signaling[11]. Previous data show that SQR inhibition attenuated hypertrophy, lung congestion, LV dilatation and myocardial fibrosis in HFrEF[64]. Future studies should explore the potential of SQR inhibitors as a therapeutic strategy for HFpEF.

While previous investigations have primarily focused on H_2S effects within single organ systems, our findings underscore the importance of considering systemic dysregulated H_2S signaling in HFpEF. The pleiotropic nature of H_2S suggests that multiple mechanisms may contribute to the observed phenotype. The recent successes of sodium-glucose cotransporter 2 inhibitors and glucagon-like peptide 1 receptor agonists in HFpEF trials further emphasize the metabolic underpinnings of this condition[65,66]. Cardiac metabolic inflexibility, characterized by impaired utilization of fatty acids and branched-chain amino acids (BCAAs), has been proposed as a key mediator of HFpEF pathology[67]. H_2S facilitates cardiac BCAA catabolism in HFrEF and is attributed to the presence of mitochondrial H_2S through 3-MST[18]. Mitochondrial H_2S is also important in maintaining mitochondrial integrity and facilitating fatty acid oxidation. 3-MST KO mice fed a 45% high fat diet were shown to have increased weight gain, adiposity, cellular lipid accumulation, glucose intolerance and overall mitochondrial dysfunction compared to their wild-type counterparts[68]. While CSE was primarily investigated in this study, the role of mitochondrial H_2S and 3-MST in HFpEF is still unknown and should be investigated further.

Our studies also reveal that peripheral organ metabolism significantly influences HFpEF pathology. We found the highest concentrations of sulfane sulfur in the liver of ZSF1 Ob rats, while hepatic lipid accumulation was notably reduced following JK-1 treatment. Given that the liver houses the majority of H_2S-generating enzymes and interfaces directly with gut-derived sulfur species, it is a pivotal mediator of H_2S homeostasis[44]. Interestingly, 10-25% of the hepatic proteins are basally sulfhydrated[20]. The role of dysregulated hepatic function, in conditions such as NAFLD and HFpEF could provide rationale to target the liver for HFpEF therapy. Emphasis on the role of NAFLD in HFpEF is increasing considering the similarities between NAFLD and cardiometabolic HFpEF along with NAFLD being shown as an independent predictor of HFpEF diagnosis irrespective of their shared comorbidities[22,39,69]. Interestingly, a study of HFpEF patients with biopsy-proven NAFLD versus non-NAFLD HFpEF patients, perturbations in cysteine metabolites were identified as a significant pathway affected in NAFLD-associated HFpEF[70]. Cysteine is a pivotal component of H_2S production, and the lack of available substrate or insufficient catabolism of H_2S-generating substrates could be responsible for the decreases in hepatic H_2S in our study. H_2S-generating capacity and bioavailability has also been shown to be impacted in NAFLD, whereby CSE is downregulated in hepatic biopsies of NAFLD-afflicted patients[25]. In the same study, hepatocyte-specific knockout of CSE lead to exacerbated hepatic lipid accumulation and metabolic dysregulation[25]. Similarly, free-fatty acids and elevated glucose concentrations downregulate CSE expression in HepG2 cells[71]. This insidious positive feedback loop of CSE depletion leading to increased hepatic lipid content and hyperglycemia that serves to further reduce CSE production suggest an important role for maintaining hepatic H_2S homeostasis in cardiometabolic HFpEF.

STUDY LIMITATIONS

This study utilized male ZSF1 Ob rats and murine models of hypertension and obesity-induced HFpEF. While these rodent models are well-established and characterized, they primarily reflect metabolic dysfunction and blood pressure dysregulation, representing only a subset of HFpEF patients.

Additionally, the exclusive use of male rats and mice limits the generalizability of our findings. Future research should focus on investigating changes in cardiac and systemic H_2S bioavailability, as well as the effects of H_2S therapy, in female animals across various HFpEF subtypes.

Another limitation is that H_2S donor therapy was administered early in the development and progression of HFpEF. Specifically, in the murine model, the H_2S donor JK-1 was given five weeks after the initiation of L-NAME and a high-fat diet, a period during which H_2S levels remain relatively normal. To rigorously evaluate H_2S therapy's efficacy in HFpEF, future experiments should involve administering H_2S donors at later stages of HFpEF progression.

CONCLUSIONS

This study offers novel insights into the dysregulation of H_2S in cardiometabolic HFpEF. We observed significant reductions in H_2S and sulfane sulfur levels in circulation, as well as in myocardial, hepatic, and renal tissues across multiple clinically relevant HFpEF models. These decreases are primarily attributed to diminished CSE expression and activity and increased SQR expression. Furthermore, enhancing H_2S bioavailability through pharmacological administration markedly improved the HFpEF phenotype.

Future research should focus on the organ-specific effects of H_2S modulation through genetic models targeting CSE, 3-MST, and SQR, as well as the precise mechanisms underlying the global and local benefits of H_2S donation in HFpEF. Additionally, the efficacy of SQR inhibitors in HFpEF should be explored.

Given that cardiometabolic HFpEF is characterized by multi-organ dysfunction, there is an urgent need for innovative therapeutic strategies and a deeper understanding of its pathophysiological drivers. Our findings strongly support a central role for H_2S deficiency in the pathology of cardiometabolic HFpEF, highlighting the necessity for further investigation into the role of H_2S in this condition.

Clinical Perspectives

Clinical competencies: This study highlights the critical role of hydrogen sulfide (H_2S) in heart failure with preserved ejection fraction (HFpEF), underscoring several key competencies for clinicians. First, healthcare providers should recognize the potential for H_2S deficiency in HFpEF patients, as this deficiency may contribute to disease progression and poor outcomes. Understanding the underlying pathophysiology—specifically the decreased production of H_2S by cystathionine-γ-lyase (CSE) and its increased metabolism by sulfide quinone oxidoreductase (SQR)—can inform treatment strategies. Additionally, the findings suggest that pharmacological H_2S supplementation may improve diastolic function and reduce cardiac fibrosis, encouraging clinicians to consider emerging therapies that target H_2S bioavailability. This study ultimately emphasizes the importance of a holistic approach to managing HFpEF, integrating metabolic and inflammatory factors alongside traditional cardiac care. **Translational Outlook:** While the study offers promising insights, several barriers must be addressed for successful clinical translation. Further research is needed to establish optimal dosing, delivery methods, and long-term safety of H_2S donors in HFpEF patients. It is also crucial to explore how individual patient characteristics, including comorbidities and genetic factors, influence H_2S metabolism and response to therapy. Robust clinical trials are essential to validate the efficacy of H_2S supplementation across diverse populations with HFpEF, ensuring that findings are generalizable. Lastly, the integration of H_2S-related interventions into existing clinical guidelines for HFpEF management will require collaboration among researchers, clinicians, and guideline committees. By addressing these barriers, future research can enhance clinical practice and improve outcomes for patients with HFpEF.

Acknowledgements: We thank Alexandra Nevins, Silpa Arkat, and Cell Biology and Bioimaging Core at Pennington Biomedical Research Center for technical support.

Data Sharing Statement: The data underlying this article will be shared on reasonable request to the corresponding author.

REFERENCES

1. Savarese G, Becher PM, Lund LH, Seferovic P, Rosano GMC, Coats AJS. Global burden of heart failure: a comprehensive and updated review of epidemiology. *Cardiovasc Res*. 2023;118:3272-3287. doi: 10.1093/cvr/cvac013

2. Loop MS, Van Dyke MK, Chen L, Brown TM, Durant RW, Safford MM, Levitan EB. Comparison of Length of Stay, 30-Day Mortality, and 30-Day Readmission Rates in Medicare Patients With Heart Failure and With Reduced Versus Preserved Ejection Fraction. *Am J Cardiol*. 2016;118:79-85. doi: 10.1016/j.amjcard.2016.04.015

3. Pfeffer MA, Shah AM, Borlaug BA. Heart Failure With Preserved Ejection Fraction In Perspective. *Circulation Research*. 2019;124:1598-1617. doi: 10.1161/circresaha.119.313572

4. Shah SJ, Borlaug BA, Kitzman DW, McCulloch AD, Blaxall BC, Agarwal R, Chirinos JA, Collins S, Deo RC, Gladwin MT, et al. Research Priorities for Heart Failure With Preserved Ejection Fraction. *Circulation*. 2020;141:1001-1026. doi: 10.1161/circulationaha.119.041886

5. Schiattarella GG, Altamirano F, Tong D, French KM, Villalobos E, Kim SY, Luo X, Jiang N, May HI, Wang ZV, et al. Nitrosative stress drives heart failure with preserved ejection fraction. *Nature*. 2019;568:351-356. doi: 10.1038/s41586-019-1100-z

6. Cruz L, Ryan JJ. Nitric Oxide Signaling in Heart Failure With Preserved Ejection Fraction. *JACC Basic Transl Sci*. 2017;2:341-343. doi: 10.1016/j.jacbts.2017.05.004

7. Abe K, Kimura H. The possible role of hydrogen sulfide as an endogenous neuromodulator. *The Journal of Neuroscience*. 1996;16:1066-1071. doi: 10.1523/jneurosci.16-03-01066.1996

8. Zhao W, Zhang J, Lu Y, Wang R. The vasorelaxant effect of H(2)S as a novel endogenous gaseous K(ATP) channel opener. *EMBO J*. 2001;20:6008-6016. doi: 10.1093/emboj/20.21.6008

9. Yang G, Wu L, Jiang B, Yang W, Qi J, Cao K, Meng Q, Mustafa AK, Mu W, Zhang S, et al. H2S as a Physiologic Vasorelaxant: Hypertension in Mice with Deletion of Cystathionine γ-Lyase. *Science*. 2008;322:587-590. doi: 10.1126/science.1162667

10. Peleli M, Bibli SI, Li Z, Chatzianastasiou A, Varela A, Katsouda A, Zukunft S, Bucci M, Vellecco V, Davos CH, et al. Cardiovascular phenotype of mice lacking 3-mercaptopyruvate sulfurtransferase. *Biochem Pharmacol*. 2020;176:113833. doi: 10.1016/j.bcp.2020.113833

11. Cirino G, Szabo C, Papapetropoulos A. Physiological roles of hydrogen sulfide in mammalian cells, tissues, and organs. *Physiol Rev*. 2023;103:31-276. doi: 10.1152/physrev.00028.2021

12. Lapenna KB, Polhemus DJ, Doiron JE, Hidalgo HA, Li Z, Lefer DJ. Hydrogen Sulfide as a Potential Therapy for Heart Failure—Past, Present, and Future. *Antioxidants*. 2021;10:485. doi: 10.3390/antiox10030485

13. Wang R. Roles of Hydrogen Sulfide in Hypertension Development and Its Complications: What, So What, Now What. *Hypertension*. 2023;80:936-944. doi: 10.1161/hypertensionaha.122.19456

14. Polhemus DJ, Calvert JW, Butler J, Lefer DJ. The Cardioprotective Actions of Hydrogen Sulfide in Acute Myocardial Infarction and Heart Failure. *Scientifica*. 2014;2014:1-8. doi: 10.1155/2014/768607

15. Polhemus DJ, Lefer DJ. Emergence of Hydrogen Sulfide as an Endogenous Gaseous Signaling Molecule in Cardiovascular Disease. *Circulation Research*. 2014;114:730-737. doi: 10.1161/circresaha.114.300505

16. Elrod JW, Calvert JW, Morrison J, Doeller JE, Kraus DW, Tao L, Jiao X, Scalia R, Kiss L, Szabo C, et al. Hydrogen sulfide attenuates myocardial ischemia-reperfusion injury by preservation of mitochondrial function. *Proceedings of the National Academy of Sciences*. 2007;104:15560-15565. doi: 10.1073/pnas.0705891104

17. Calvert JW, Jha S, Gundewar S, Elrod JW, Ramachandran A, Pattillo CB, Kevil CG, Lefer DJ. Hydrogen sulfide mediates cardioprotection through Nrf2 signaling. *Circ Res*. 2009;105:365-374. doi: 10.1161/CIRCRESAHA.109.199919

18. Li Z, Xia H, Sharp TE, Lapenna KB, Elrod JW, Casin KM, Liu K, Calvert JW, Chau VQ, Salloum FN, et al. Mitochondrial H2S Regulates BCAA Catabolism in Heart Failure. *Circulation Research*. 2022;131:222-235. doi: 10.1161/circresaha.121.319817

19. Zanardo RCO, Brancaleone V, Distrutti E, Fiorucci S, Cirino G, Wallace JL. Hydrogen Sulfide is an Endogenous Modulator of Leukocyte-mediated Inflammation. *The FASEB Journal*. 2006;20:2118-2120. doi: https://doi.org/10.1096/fj.06-6270fje

20. Mustafa AK, Gadalla MM, Sen N, Kim S, Mu W, Gazi SK, Barrow RK, Yang G, Wang R, Snyder SH. H2S Signals Through Protein S-Sulfhydration. *Science Signaling*. 2009;2:ra72-ra72. doi: 10.1126/scisignal.2000464

21. King AL, Polhemus DJ, Bhushan S, Otsuka H, Kondo K, Nicholson CK, Bradley JM, Islam KN, Calvert JW, Tao Y-X, et al. Hydrogen sulfide cytoprotective signaling is endothelial nitric oxide synthase-nitric oxide dependent. *Proceedings of the National Academy of Sciences*. 2014;111:3182-3187. doi: 10.1073/pnas.1321871111

22. Capone F, Vettor R, Schiattarella GG. Cardiometabolic HFpEF: NASH of the Heart. *Circulation*. 2023;147:451-453. doi: doi:10.1161/CIRCULATIONAHA.122.062874

23. Shah SJ, Katz DH, Selvaraj S, Burke MA, Yancy CW, Gheorghiade M, Bonow RO, Huang C-C, Deo RC. Phenomapping for Novel Classification of Heart Failure With Preserved Ejection Fraction. *Circulation*. 2015;131:269-279. doi: 10.1161/circulationaha.114.010637

24. Cohen JB, Schrauben SJ, Zhao L, Basso MD, Cvijic ME, Li Z, Yarde M, Wang Z, Bhattacharya PT, Chirinos DA, et al. Clinical Phenogroups in Heart Failure With Preserved Ejection Fraction. *JACC: Heart Failure*. 2020;8:172-184. doi: 10.1016/j.jchf.2019.09.009

25. Xu W, Cui C, Cui C, Chen Z, Zhang H, Cui Q, Xu G, Fan J, Han Y, Tang L, et al. Hepatocellular cystathionine gamma lyase/hydrogen sulfide attenuates nonalcoholic fatty liver disease by activating farnesoid X receptor. *Hepatology*. 2022;76:1794-1810. doi: 10.1002/hep.32577

26. Barr LA, Shimizu Y, Lambert JP, Nicholson CK, Calvert JW. Hydrogen sulfide attenuates high fat diet-induced cardiac dysfunction via the suppression of endoplasmic reticulum stress. *Nitric Oxide*. 2015;46:145-156. doi: 10.1016/j.niox.2014.12.013

27. Suzuki K, Olah G, Modis K, Coletta C, Kulp G, Gerö D, Szoleczky P, Chang T, Zhou Z, Wu L, et al. Hydrogen sulfide replacement therapy protects the vascular endothelium in hyperglycemia by preserving mitochondrial function. *Proceedings of the National Academy of Sciences*. 2011;108:13829-13834. doi: 10.1073/pnas.1105121108

28. Padiya R, Khatua TN, Bagul PK, Kuncha M, Banerjee SK. Garlic improves insulin sensitivity and associated metabolic syndromes in fructose fed rats. *Nutrition & Metabolism*. 2011;8:53. doi: 10.1186/1743-7075-8-53

29. Zhong G, Chen F, Cheng Y, Tang C, Du J. The role of hydrogen sulfide generation in the pathogenesis of hypertension in rats induced by inhibition of nitric oxide synthase. *Journal of Hypertension*. 2003;21:1879-1885.

30. Li Z, Xia H, Sharp TE, Lapenna KB, Katsouda A, Elrod JW, Pfeilschifter J, Beck K-F, Xu S, Xian M, et al. Hydrogen Sulfide Modulates Endothelial–Mesenchymal Transition in Heart Failure. *Circulation Research*. 2023;132:154-166. doi: 10.1161/circresaha.122.321326

31. Kang J, Li Z, Organ CL, Park CM, Yang CT, Pacheco A, Wang D, Lefer DJ, Xian M. pH-Controlled Hydrogen Sulfide Release for Myocardial Ischemia-Reperfusion Injury. *J Am Chem Soc*. 2016;138:6336-6339. doi: 10.1021/jacs.6b01373

32. Li Z, Organ CL, Kang J, Polhemus DJ, Trivedi RK, Sharp TE, 3rd, Jenkins JS, Tao YX, Xian M, Lefer DJ. Hydrogen Sulfide Attenuates Renin Angiotensin and Aldosterone Pathological Signaling to Preserve Kidney Function and Improve Exercise Tolerance in Heart Failure. *JACC Basic Transl Sci*. 2018;3:796-809. doi: 10.1016/j.jacbts.2018.08.011

33. Li Z, Xia H, Sharp TE, 3rd, LaPenna KB, Elrod JW, Casin KM, Liu K, Calvert JW, Chau VQ, Salloum FN, et al. Mitochondrial H(2)S Regulates BCAA Catabolism in Heart Failure. *Circ Res*. 2022;131:222-235. doi: 10.1161/CIRCRESAHA.121.319817

34. Li Z, Xia H, Sharp TE, 3rd, LaPenna KB, Katsouda A, Elrod JW, Pfeilschifter J, Beck KF, Xu S, Xian M, et al. Hydrogen Sulfide Modulates Endothelial-Mesenchymal Transition in Heart Failure. *Circ Res*. 2023;132:154-166. doi: 10.1161/CIRCRESAHA.122.321326

35. Lapenna KB, Li Z, Doiron JE, Sharp TE, Xia H, Moles K, Koul K, Wang JS, Polhemus DJ, Goodchild TT, et al. Combination Sodium Nitrite and Hydralazine Therapy Attenuates Heart Failure With Preserved Ejection Fraction Severity in a “2-Hit” Murine Model. *Journal of the American Heart Association*. 2023. doi: 10.1161/jaha.122.028480

36. Mok YY, Atan MS, Yoke Ping C, Zhong Jing W, Bhatia M, Moochhala S, Moore PK. Role of hydrogen sulphide in haemorrhagic shock in the rat: protective effect of inhibitors of hydrogen sulphide biosynthesis. *Br J Pharmacol*. 2004;143:881-889. doi: 10.1038/sj.bjp.0706014

37. Xia H, Li Z, Sharp TE, Polhemus DJ, Carnal J, Moles KH, Tao YX, Elrod J, Pfeilschifter J, Beck KF, Lefer DJ. Endothelial Cell Cystathionine γ-Lyase Expression Level Modulates Exercise

Capacity, Vascular Function, and Myocardial Ischemia Reperfusion Injury. *Journal of the American Heart Association*. 2020;9. doi: 10.1161/jaha.120.017544

38. Nayor M, Houstis NE, Namasivayam M, Rouvina J, Hardin C, Shah RV, Ho JE, Malhotra R, Lewis GD. Impaired Exercise Tolerance in Heart Failure With Preserved Ejection Fraction: Quantification of Multiorgan System Reserve Capacity. *JACC Heart Fail*. 2020;8:605-617. doi: 10.1016/j.jchf.2020.03.008

39. Fudim M, Zhong L, Patel KV, Khera R, Abdelmalek MF, Diehl AM, McGarrah RW, Molinger J, Moylan CA, Rao VN, et al. Nonalcoholic Fatty Liver Disease and Risk of Heart Failure Among Medicare Beneficiaries. *J Am Heart Assoc*. 2021;10:e021654. doi: 10.1161/JAHA.121.021654

40. Roh J, Hill JA, Singh A, Valero-Muñoz M, Sam F. Heart Failure With Preserved Ejection Fraction: Heterogeneous Syndrome, Diverse Preclinical Models. *Circulation Research*. 2022;130:1906-1925. doi: 10.1161/circresaha.122.320257

41. Hamdani N, Franssen C, Lourenco A, Falcao-Pires I, Fontoura D, Leite S, Plettig L, Lopez B, Ottenheijm CA, Becher PM, et al. Myocardial titin hypophosphorylation importantly contributes to heart failure with preserved ejection fraction in a rat metabolic risk model. *Circ Heart Fail*. 2013;6:1239-1249. doi: 10.1161/CIRCHEARTFAILURE.113.000539

42. Oktay AA, Rich JD, Shah SJ. The Emerging Epidemic of Heart Failure with Preserved Ejection Fraction. *Current Heart Failure Reports*. 2013;10:401-410. doi: 10.1007/s11897-013-0155-7

43. Tsao CW, Aday AW, Almarzooq ZI, Anderson CAM, Arora P, Avery CL, Baker-Smith CM, Beaton AZ, Boehme AK, Buxton AE, et al. Heart Disease and Stroke Statistics-2023 Update: A

Report From the American Heart Association. *Circulation*. 2023;147:e93-e621. doi: 10.1161/CIR.0000000000001123

44. Cirino G, Szabo C, Papapetropoulos A. Physiological roles of hydrogen sulfide in mammalian cells, tissues, and organs. *Physiological Reviews*. 2023;103:31-276. doi: 10.1152/physrev.00028.2021

45. Cheng Y, Ndisang JF, Tang G, Cao K, Wang R. Hydrogen sulfide-induced relaxation of resistance mesenteric artery beds of rats. *Am J Physiol Heart Circ Physiol*. 2004;287:H2316-2323. doi: 10.1152/ajpheart.00331.2004

46. Coletta C, Papapetropoulos A, Erdelyi K, Olah G, Modis K, Panopoulos P, Asimakopoulou A, Gero D, Sharina I, Martin E, Szabo C. Hydrogen sulfide and nitric oxide are mutually dependent in the regulation of angiogenesis and endothelium-dependent vasorelaxation. *Proc Natl Acad Sci U S A*. 2012;109:9161-9166. doi: 10.1073/pnas.1202916109

47. Greaney JL, Kutz JL, Shank SW, Jandu S, Santhanam L, Alexander LM. Impaired Hydrogen Sulfide-Mediated Vasodilation Contributes to Microvascular Endothelial Dysfunction in Hypertensive Adults. *Hypertension*. 2017;69:902-909. doi: 10.1161/HYPERTENSIONAHA.116.08964

48. Altaany Z, Yang G, Wang R. Crosstalk between hydrogen sulfide and nitric oxide in endothelial cells. *J Cell Mol Med*. 2013;17:879-888. doi: 10.1111/jcmm.12077

49. Saha S, Chakraborty PK, Xiong X, Dwivedi SK, Mustafi SB, Leigh NR, Ramchandran R, Mukherjee P, Bhattacharya R. Cystathionine beta-synthase regulates endothelial function via protein S-sulfhydration. *FASEB J*. 2016;30:441-456. doi: 10.1096/fj.15-278648

50. Bibli SI, Hu J, Sigala F, Wittig I, Heidler J, Zukunft S, Tsilimigras DI, Randriamboavonjy V, Wittig J, Kojonazarov B, et al. Cystathionine gamma Lyase Sulfhydrates the RNA Binding Protein Human Antigen R to Preserve Endothelial Cell Function and Delay Atherogenesis. *Circulation*. 2019;139:101-114. doi: 10.1161/CIRCULATIONAHA.118.034757

51. Cheung SH, Kwok WK, To KF, Lau JY. Anti-atherogenic effect of hydrogen sulfide by over-expression of cystathionine gamma-lyase (CSE) gene. *PLoS One*. 2014;9:e113038. doi: 10.1371/journal.pone.0113038

52. Mani S, Li H, Untereiner A, Wu L, Yang G, Austin RC, Dickhout JG, Lhotak S, Meng QH, Wang R. Decreased endogenous production of hydrogen sulfide accelerates atherosclerosis. *Circulation*. 2013;127:2523-2534. doi: 10.1161/CIRCULATIONAHA.113.002208

53. Zhang H, Guo C, Wu D, Zhang A, Gu T, Wang L, Wang C. Hydrogen sulfide inhibits the development of atherosclerosis with suppressing CX3CR1 and CX3CL1 expression. *PLoS One*. 2012;7:e41147. doi: 10.1371/journal.pone.0041147

54. Calvert JW, Elston M, Nicholson CK, Gundewar S, Jha S, Elrod JW, Ramachandran A, Lefer DJ. Genetic and pharmacologic hydrogen sulfide therapy attenuates ischemia-induced heart failure in mice. *Circulation*. 2010;122:11-19. doi: 10.1161/CIRCULATIONAHA.109.920991

55. King AL, Polhemus DJ, Bhushan S, Otsuka H, Kondo K, Nicholson CK, Bradley JM, Islam KN, Calvert JW, Tao YX, et al. Hydrogen sulfide cytoprotective signaling is endothelial nitric oxide synthase-nitric oxide dependent. *Proc Natl Acad Sci U S A*. 2014;111:3182-3187. doi: 10.1073/pnas.1321871111

56. Kondo K, Bhushan S, King AL, Prabhu SD, Hamid T, Koenig S, Murohara T, Predmore BL, Gojon G, Sr., Gojon G, Jr., et al. H(2)S protects against pressure overload-induced heart failure via upregulation of endothelial nitric oxide synthase. *Circulation*. 2013;127:1116-1127. doi: 10.1161/CIRCULATIONAHA.112.000855

57. Polhemus D, Kondo K, Bhushan S, Bir SC, Kevil CG, Murohara T, Lefer DJ, Calvert JW. Hydrogen sulfide attenuates cardiac dysfunction after heart failure via induction of angiogenesis. *Circ Heart Fail*. 2013;6:1077-1086. doi: 10.1161/CIRCHEARTFAILURE.113.000299

58. Altaany Z, Ju Y, Yang G, Wang R. The coordination of S-sulfhydration, S-nitrosylation, and phosphorylation of endothelial nitric oxide synthase by hydrogen sulfide. *Science Signaling*. 2014;7:ra87-ra87. doi: doi:10.1126/scisignal.2005478

59. Armstrong PW, Lam CSP, Anstrom KJ, Ezekowitz J, Hernandez AF, O'Connor CM, Pieske B, Ponikowski P, Shah SJ, Solomon SD, et al. Effect of Vericiguat vs Placebo on Quality of Life in Patients With Heart Failure and Preserved Ejection Fraction. *JAMA*. 2020;324:1512. doi: 10.1001/jama.2020.15922

60. Redfield MM, Chen HH, Borlaug BA, Semigran MJ, Lee KL, Lewis G, Lewinter MM, Rouleau JL, Bull DA, Mann DL, et al. Effect of Phosphodiesterase-5 Inhibition on Exercise Capacity and

Clinical Status in Heart Failure With Preserved Ejection Fraction. *JAMA*. 2013;309:1268. doi: 10.1001/jama.2013.2024

61. Borlaug BA, Anstrom KJ, Lewis GD, Shah SJ, Levine JA, Koepp GA, Givertz MM, Felker GM, Lewinter MM, Mann DL, et al. Effect of Inorganic Nitrite vs Placebo on Exercise Capacity Among Patients With Heart Failure With Preserved Ejection Fraction. *JAMA*. 2018;320:1764. doi: 10.1001/jama.2018.14852

62. Stolina M, Luo X, Dwyer D, Han C-Y, Chen R, Zhang Y, Xiong Y, Chen Y, Yin J, Shkumatov A, et al. The evolving systemic biomarker milieu in obese ZSF1 rat model of human cardiometabolic syndrome: Characterization of the model and cardioprotective effect of GDF15. *PLOS ONE*. 2020;15:e0231234. doi: 10.1371/journal.pone.0231234

63. Borges Canha M, Portela-Cidade JP, Conceicao G, Sousa-Mendes C, Leite S, Fontoura D, Moreira-Goncalves D, Falcao-Pires I, Lourenco A, Leite-Moreira A, Pimentel-Nunes P. Characterization of liver changes in ZSF1 rats, an animal model of metabolic syndrome. *Rev Esp Enferm Dig*. 2017;109:491-497. doi: 10.17235/reed.2017.4575/2016

64. Jackson MR, Cox KD, Baugh SDP, Wakeen L, Rashad AA, Lam PYS, Polyak B, Jorns MS. Discovery of a first-in-class inhibitor of sulfide:quinone oxidoreductase that protects against adverse cardiac remodelling and heart failure. *Cardiovasc Res*. 2022;118:1771-1784. doi: 10.1093/cvr/cvab206

65. Butler J, Filippatos G, Jamal Siddiqi T, Brueckmann M, Böhm M, Chopra VK, Pedro Ferreira J, Januzzi JL, Kaul S, Piña IL, et al. Empagliflozin, Health Status, and Quality of Life in Patients

With Heart Failure and Preserved Ejection Fraction: The EMPEROR-Preserved Trial. *Circulation*. 2022;145:184-193. doi: 10.1161/circulationaha.121.057812

66. Kosiborod MN, Abildstrom SZ, Borlaug BA, Butler J, Rasmussen S, Davies M, Hovingh GK, Kitzman DW, Lindegaard ML, Moller DV, et al. Semaglutide in Patients with Heart Failure with Preserved Ejection Fraction and Obesity. *N Engl J Med*. 2023. doi: 10.1056/NEJMoa2306963

67. Hahn VS, Petucci C, Kim MS, Bedi KC, Jr., Wang H, Mishra S, Koleini N, Yoo EJ, Margulies KB, Arany Z, et al. Myocardial Metabolomics of Human Heart Failure With Preserved Ejection Fraction. *Circulation*. 2023;147:1147-1161. doi: 10.1161/CIRCULATIONAHA.122.061846

68. Katsouda A, Valakos D, Dionellis VS, Bibli SI, Akoumianakis I, Karaliota S, Zuhra K, Fleming I, Nagahara N, Havaki S, et al. MPST sulfurtransferase maintains mitochondrial protein import and cellular bioenergetics to attenuate obesity. *J Exp Med*. 2022;219. doi: 10.1084/jem.20211894

69. Salah HM, Pandey A, Soloveva A, Abdelmalek MF, Diehl AM, Moylan CA, Wegermann K, Rao VN, Hernandez AF, Tedford RJ, et al. Relationship of Nonalcoholic Fatty Liver Disease and Heart Failure With Preserved Ejection Fraction. *JACC Basic Transl Sci*. 2021;6:918-932. doi: 10.1016/j.jacbts.2021.07.010

70. Wegermann K, Fudim M, Henao R, Howe CF, McGarrah R, Guy C, Abdelmalek MF, Diehl AM, Moylan CA. Serum Metabolites Are Associated With HFpEF in Biopsy-Proven Nonalcoholic Fatty Liver Disease. *Journal of the American Heart Association*. 2023;12. doi: 10.1161/jaha.123.029873

71. Ali A, Zhang Y, Fu M, Pei Y, Wu L, Wang R, Yang G. Cystathionine gamma-lyase/H(2)S system suppresses hepatic acetyl-CoA accumulation and nonalcoholic fatty liver disease in mice. *Life Sci*. 2020;252:117661. doi: 10.1016/j.lfs.2020.117661

Table 1. Baseline Characteristics of participants with HFpEF vs. Healthy Controls.

Characteristics	All participants (N=96)	Controls (N=48)	Participants with HFpEF (N=48)	P value
Age, mean ± SD, years	61 ± 13	61 ± 13	62 ± 14	0.85
Male sex, n (%)	36 (37.5)	18 (37.5)	18 (37.5)	1.00
White race, n (%)	80 (83.3)	40 (83.3)	40 (83.3)	1.00
Hypertension, n (%)	49 (51.0)	19 (39.6)	30 (62.5)	0.04
Diabetes, n (%)	15 (15.6)	8 (16.7)	7 (14.6)	1.00
Hypercholesterolemia, n (%)	55 (57.3)	27 (56.2)	28 (58.3)	1.00
Coronary artery disease, n (%)	12 (12.5)	2 (4.2)	10 (20.8)	0.03
BMI, median (IQR), kg/m^2	30.3 (26.0- 35.7)	27.7 (24.9- 32.4)	31.0 (28.3- 38.9)	<0.01
HDL, median (IQR), mg/dL	53 (43- 63)	59 (48- 70)	49 (42- 56)	<0.01
LDL, median (IQR), mg/dL	108 (83- 141)	129 (102- 161)	96 (68- 116)	<0.01
Creatinine, median (IQR), mg/dL	0.9 (0.8- 1.1)	0.9 (0.8- 1.0)	0.9 (0.8- 1.1)	0.83
Glucose, median (IQR), mg/dL	101 (93- 109)	101 (94 - 108)	102 (91- 109)	0.88
Triglycerides,median (IQR), mg/dL	125 (83- 172)	108 (80- 149)	144 (92- 206)	0.02
LVEF, median (IQR), %	60 (56- 65)	63 (58- 66)	58 (51- 63)	<0.01
ACE inhibitors, n (%)	24 (25.0)	6 (12.5)	18 (37.5)	0.01
Beta blockers, n (%)	39 (40.6)	4 (8.3)	35 (72.9)	<0.01
Statin, n (%)	42 (43.8)	18 (37.5)	24 (50.0)	0.30
Aspirin, n (%)	40 (41.7)	23 (47.9)	17 (35.4)	0.30

The Wilcoxon–rank sum test or Welch two sample t-test for continuous variables and the $\chi 2$ test or Fisher's exact test for categorical variables were used to determine significant difference between groups. Abbreviations: ACE, angiotensin converting enzyme; BMI, body mass index; HDL, high-density lipoprotein; IQR, interquartile range; LDL, low-density lipoprotein; LVEF, left ventricular ejection fraction

FIGURE LEGENDS

Figure 1. Reduced Circulating Hydrogen Sulfide in HFpEF Patients.

(A) Measurement of H_2S, sulfane sulfur and hs-CRP in plasma from control and HFpEF patients ***(B)*** Circulating H_2S, ***(C)*** Circulating sulfane sulfur, ***(D)*** Circulating hs-CRP. Circled number inside bars indicate sample size. Data in panels ***B-D*** were analyzed with Student unpaired 2-tail *t* test. Data are presented as box plots (median, minimum, and maximum). ELISA, enzyme-linked immunosorbent assay; GC, gas chromatography; Hs-CRP, high-sensitivity C-reactive protein.

Figure 2. HFpEF Pathology in "Two-hit" Murine HFpEF Model.

(***A***) Study timeline, (***B***) Body weight, (***C***) Systolic blood pressure, (***D***) Diastolic blood pressure, ***(E)*** Left ventricular ejection fraction (LVEF), ***(F)*** Ratio of early mitral diastolic inflow velocity (E) and mitral annular early diastolic velocity (e'), (***G***) Left ventricular end diastolic pressure (LVEDP), ***(H)*** Treadmill exercise distance, ***(I)*** Aortic vascular reactivity to acetylcholine (ACh), ***(J)*** Aortic vascular reactivity to sodium nitroprusside (SNP). Data in panel ***B*** was analyzed with Student unpaired 2-tail *t* test. Data in panels ***B-H*** were analyzed with multiple Student unpaired 2-tail *t* tests. Data in panels ***I*** and ***J*** were analyzed with ordinary 2-way ANOVA. Data in panels ***B-G*** are presented as box plots (median, minimum, and maximum). Data in panels ***H-J*** are presented as mean ± SEM.

Figure 3. Circulating and Myocardial Hydrogen Sulfide Bioavailability in "Two-hit" Murine HFpEF Model.

(***A***) Circulating H_2S, ***(B)*** Circulating sulfane sulfur, ***(C)*** Myocardial H_2S, ***(D)*** Myocardial sulfane sulfur, ***(E)*** Myocardial CSE gene expression, ***(F)*** Myocardial CSE protein expression, ***(G)*** Myocardial CSE enzyme activity, ***(H)*** Myocardial SQR gene expression, ***(I)*** Myocardial SQR protein expression. Data in panels ***A-D*** were analyzed with multiple Student unpaired 2-tail *t* tests. Data in panels ***E-I*** were

analyzed with Student unpaired 2-tail *t* tests. Data are presented as box plots (median, minimum, and maximum).. CSE, cystathionine γ-lyase; SQR, sulfide quinone oxidoreductase.

Figure 4. Increased HFpEF Severity in Endothelial Cell (EC) Cystathionine Gamma Lyase (CSE) Knockout Mice.

(***A***) Study timeline, (***B***) Circulating H_2S, ***(C)*** Circulating sulfane sulfur, ***(D)*** Myocardial H_2S, ***(E)*** Myocardial sulfane sulfur, ***(F)*** Left ventricular ejection fraction (LVEF), ***(G)*** Ratio of early mitral diastolic inflow velocity (E) and mitral annular early diastolic velocity (e'), (***H***) Left ventricular end diastolic pressure (LVEDP), ***(I)*** Treadmill exercise distance, ***(J)*** Aortic vascular reactivity to acetylcholine (ACh), ***(K)*** Aortic vascular reactivity to sodium nitroprusside (SNP), ***(L)*** Survival analysis. Data in panels ***B-E*** and ***H*** were analyzed with Student unpaired 2-tail *t* test. Data in panels ***F, G*** and ***I*** were analyzed with Student unpaired 2-tail *t* test. Data in panels ***J*** and ***K*** were analyzed with ordinary 2-way ANOVA. Survival data in panel ***L*** was analyzed with Kaplan-Meier survival analysis. Data in panels ***B-H*** are presented as box plots (median, minimum, and maximum). Data in panels ***I-K*** are presented as mean ± SEM. * Echocardiography, # Treadmill exercise, ♀ Aortic vascular reactivity, Invasive hemodynamics, H_2S and sulfane sulfur measurements.

Figure 5. Hydrogen Sulfide Therapy Attenuates HFpEF Severity in Murine "Two-Hit" Model.

(***A***) Study timeline, (***B***) Circulating H_2S, ***(C)*** Circulating sulfane sulfur, ***(D)*** Myocardial H_2S, ***(E)*** Myocardial sulfane sulfur, (***F***) Systolic blood pressure, (***G***) Diastolic blood pressure, ***(H)*** Ratio of early mitral diastolic inflow velocity (E) and mitral annular early diastolic velocity (e'), (***I***) Left ventricular end diastolic pressure (LVEDP), ***(J)*** Treadmill exercise distance, ***(K)*** Representative images of cardiac interstitial fibrosis in HFpEF (upper) and HFpEF + JK-1 (lower) animals stained with Masson's Trichrome and respective quantification, (***L***) Representative images of cardiac perivascular fibrosis

stained with Masson's Trichrome and respective quantification, (***M***) Representative images of hepatic lipid accumulation stained with hematoxylin and eosin and respective quantification. Data were analyzed with Student unpaired 2-tail *t* test. Data in all panels are presented as box plots (median, minimum, and maximum) except data in panel ***J*** are presented as mean ± SEM. * Echocardiography and Treadmill exercise, ♀ Invasive hemodynamics, H_2S and sulfane sulfur measurements, Cardiac fibrosis and hepatic lipid content.

Figure 6. Reduced Circulating Hydrogen Sulfide Bioavailability and HFpEF Severity in the ZSF1 Obese Rat

(A) Study Timeline, (***B***) Body weight, ***(C)*** Non-fasting blood glucose, (***D***) Systolic blood pressure, ***(E)*** Diastolic blood pressure, ***(F)*** Left ventricular ejection fraction (LVEF), ***(G)*** Ratio of early mitral diastolic inflow velocity (E) and mitral annular early diastolic velocity (e'), (***H***) Left ventricular end diastolic pressure (LVEDP), ***(I)*** Treadmill exercise distance, (***J***) Circulating H_2S, ***(K)*** Circulating sulfane sulfur. Data in panels ***B, C, F, G, I-K*** were analyzed with multiple Student unpaired 2-tail *t* tests. Data in panels ***D, E and H*** were analyzed with Student unpaired 2-tail *t* test. Data are presented as mean ± SEM.

Figure 7. Reduced Expression of CSE and Increased Expression of SQR in the ZSF1 Obese Rat Tissues.

(A) Myocardial CSE gene expression, (***B***) Myocardial CSE protein expression, ***(C)*** Myocardial SQR gene expression, (***D***) Myocardial SQR protein expression, ***(E)*** Hepatic CSE gene expression, (***F***) Hepatic CSE protein expression, ***(G)*** Hepatic SQR gene expression, ***(H)*** Hepatic SQR protein expression, ***(I)*** Renal CSE gene expression, (***J***) Renal CSE protein expression, ***(K)*** Renal SQR gene expression, ***(L)*** Renal SQR protein expression. Data were analyzed with Student unpaired 2-tail *t* test. Data are presented

as box plots (median, minimum, and maximum). CSE, cystathionine γ-lyase; SQR, sulfide quinone oxidoreductase.

Figure 8. Histopathological Changes and Reduced Hydrogen Sulfide and CSE Enzyme Activity in the ZSF1 Obese Rat Tissues.

(***A***) Representative images of cardiac perivascular fibrosis stained with Masson's Trichrome and fast green counterstaining and respective quantification, (***B***) Myocardial H_2S, ***(C)*** Myocardial CSE enzyme activity, ***(D)*** Representative images of hepatic lipid accumulation stained with hematoxylin and eosin and respective quantification, ***(E)*** Hepatic H_2S, (***F***) Hepatic CSE enzyme activity, (***G***) Representative images of renal perivascular fibrosis stained with Masson's Trichrome and fast green counterstaining and respective quantification, ***(H)*** Renal H_2S, (***I***) Renal CSE enzyme activity. Data in panels ***A, B, D, E, G and H*** were analyzed with multiple Student unpaired 2-tail *t* tests. Data in panels ***C, F and I*** were analyzed with Student unpaired 2-tail *t* test. Data are presented as mean ± SEM. CSE, cystathionine γ-lyase.

Figure 1

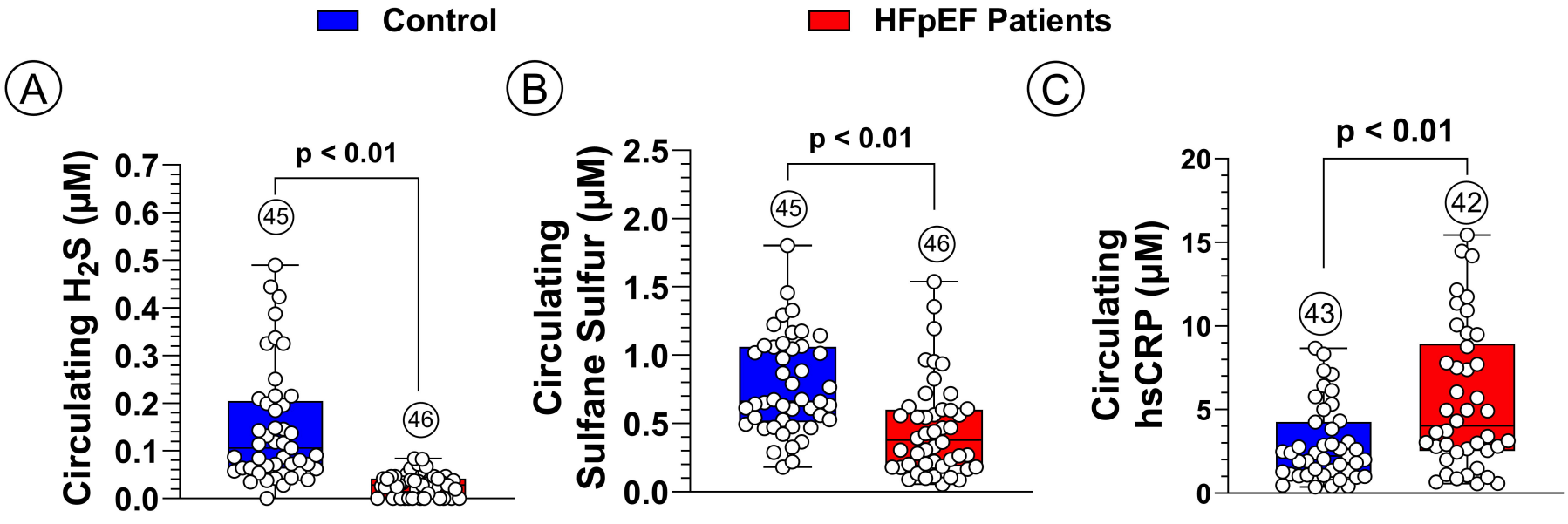
Control
HFpEF Patients
A
Circulating H_2S (μM)
0.7
0.6
0.5
0.4
0.3
0.2
0.1
0.0
p < 0.01
45
46
B
Circulating Sulfane Sulfur (μM)
2.5
2.0
1.5
1.0
0.5
0.0
p < 0.01
45
46
C
Circulating hsCRP (μM)
20
15
10
5
0
p < 0.01
43
42

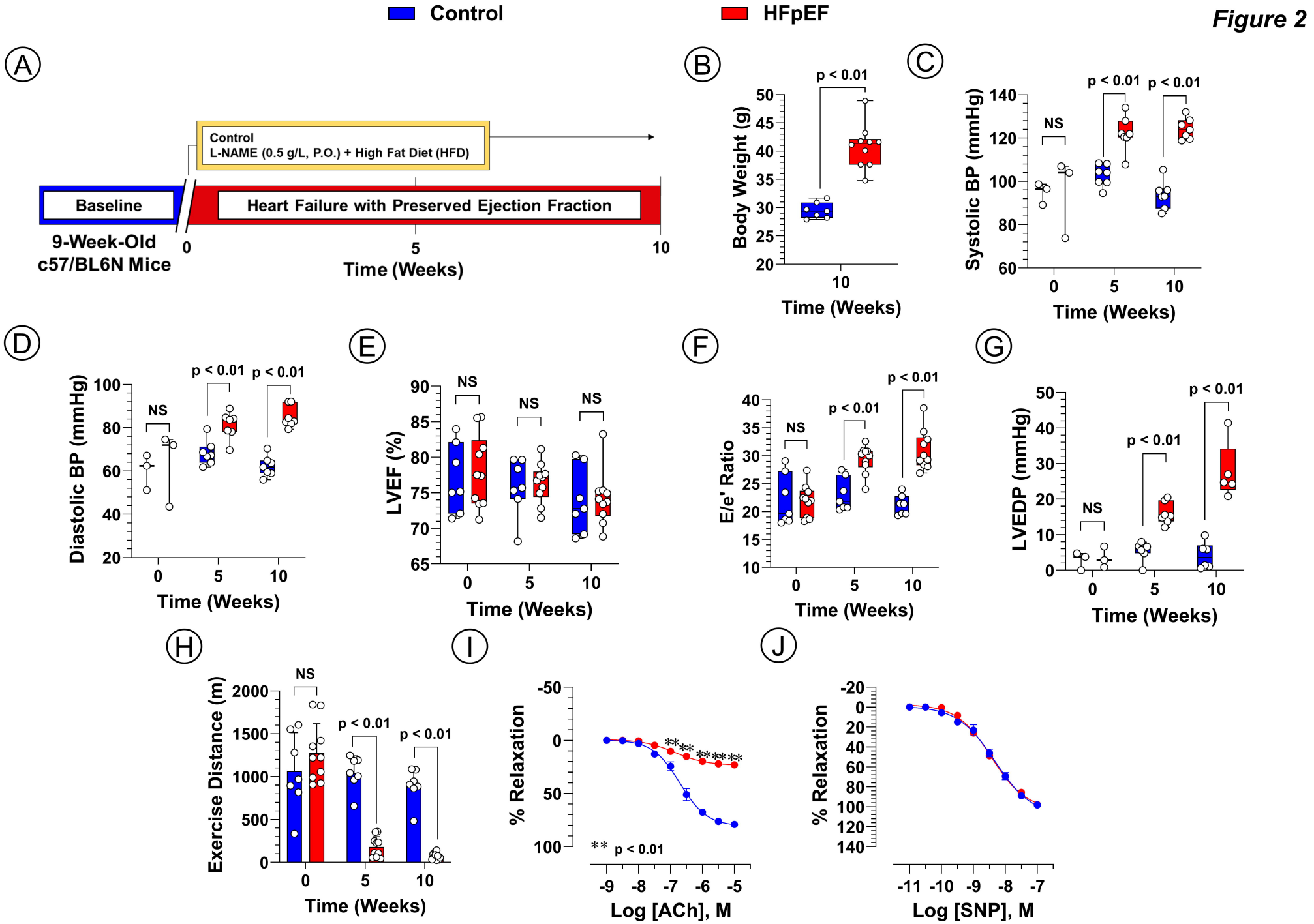
Figure 2
Control
HFpEF
A
Control
L-NAME (0.5 g/L, P.O.) + High Fat Diet (HFD)
Baseline
Heart Failure with Preserved Ejection Fraction
9-Week-Old
c57/BL6N Mice
0
5
10
Time (Weeks)
B
Body Weight (g)
p < 0.01
Time (Weeks)
C
Systolic BP (mmHg)
NS
p < 0.01
p < 0.01
Time (Weeks)
D
Diastolic BP (mmHg)
NS
p < 0.01
p < 0.01
Time (Weeks)
E
LVEF (%)
NS
NS
NS
Time (Weeks)
F
E/e' Ratio
NS
p < 0.01
p < 0.01
Time (Weeks)
G
LVEDP (mmHg)
NS
p < 0.01
p < 0.01
Time (Weeks)
H
Exercise Distance (m)
NS
p < 0.01
p < 0.01
Time (Weeks)
I
% Relaxation
** p < 0.01
Log [ACh], M
J
% Relaxation
Log [SNP], M

Figure 3

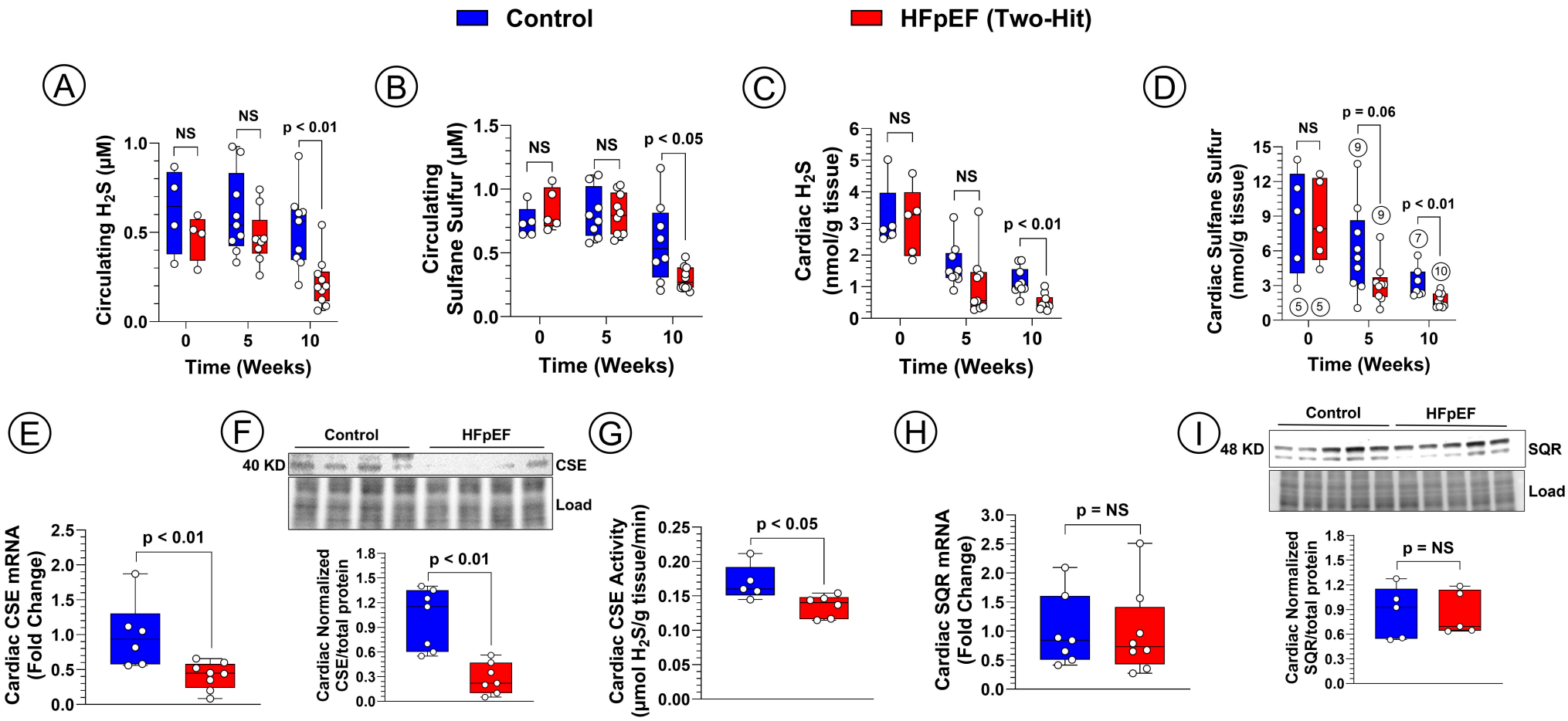
Control
HFpEF (Two-Hit)
A
Circulating H2S (µM)
NS
NS
p < 0.01
Time (Weeks)
B
Circulating Sulfane Sulfur (µM)
NS
NS
p < 0.05
Time (Weeks)
C
Cardiac H2S (nmol/g tissue)
NS
NS
p < 0.01
Time (Weeks)
D
Cardiac Sulfane Sulfur (nmol/g tissue)
NS
p = 0.06
p < 0.01
Time (Weeks)
E
Cardiac CSE mRNA (Fold Change)
p < 0.01
F
Control
HFpEF
40 KD
CSE
Load
Cardiac Normalized CSE/total protein
p < 0.01
G
Cardiac CSE Activity (µmol H2S/g tissue/min)
p < 0.05
H
Cardiac SQR mRNA (Fold Change)
p = NS
I
Control
HFpEF
48 KD
SQR
Load
Cardiac Normalized SQR/total protein
p = NS

Figure 4

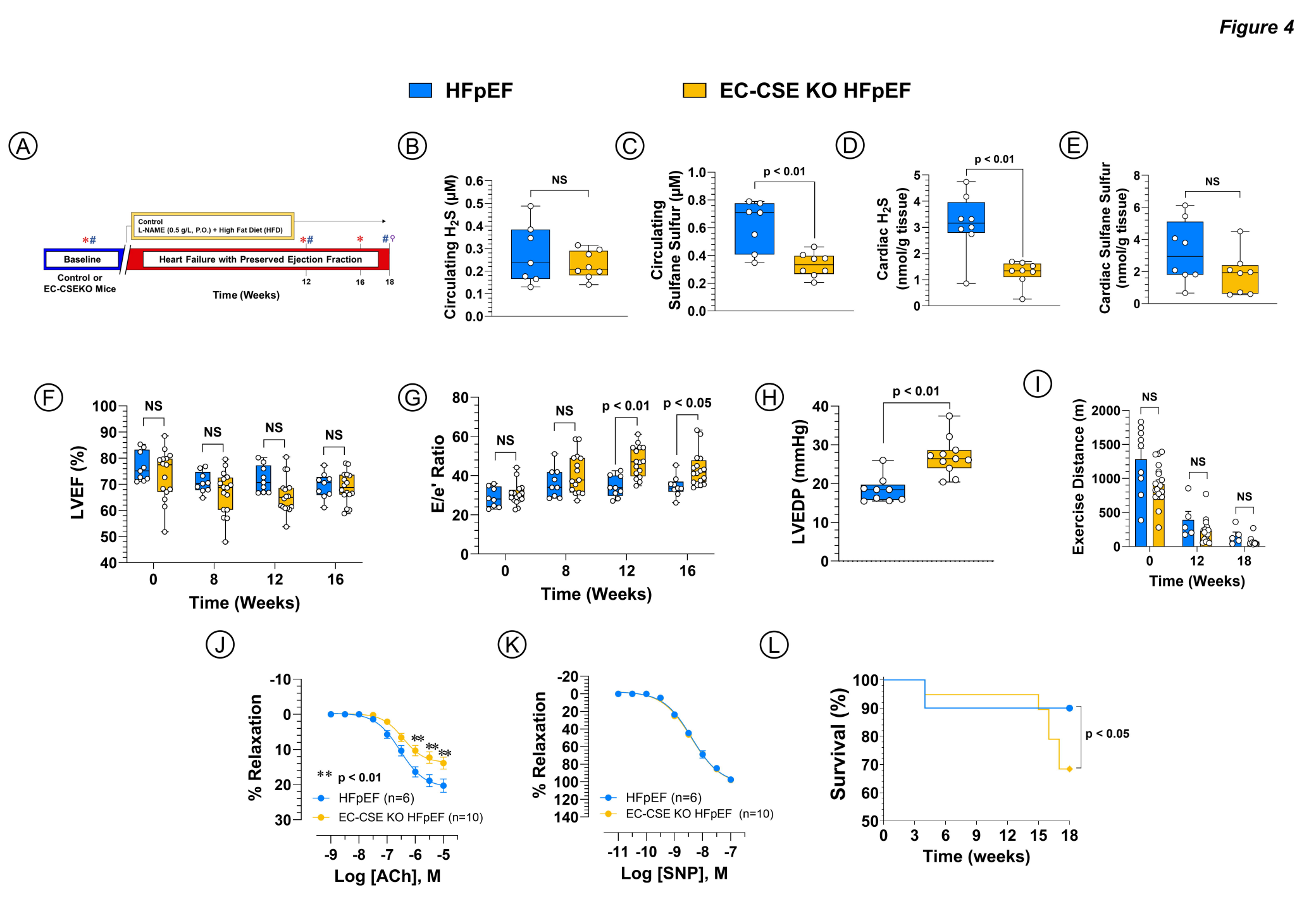
HFpEF
EC-CSE KO HFpEF
A
Control
L-NAME (0.5 g/L, P.O.) + High Fat Diet (HFD)
Baseline
Control or
EC-CSEKO Mice
Heart Failure with Preserved Ejection Fraction
Time (Weeks)
B
Circulating H2S (μM)
NS
C
Circulating Sulfane Sulfur (μM)
p < 0.01
D
Cardiac H2S (nmol/g tissue)
p < 0.01
E
Cardiac Sulfane Sulfur (nmol/g tissue)
NS
F
LVEF (%)
NS
Time (Weeks)
G
E/e' Ratio
NS
p < 0.01
p < 0.05
Time (Weeks)
H
LVEDP (mmHg)
p < 0.01
I
Exercise Distance (m)
NS
Time (Weeks)
J
% Relaxation
** p < 0.01
HFpEF (n=6)
EC-CSE KO HFpEF (n=10)
Log [ACh], M
K
% Relaxation
HFpEF (n=6)
EC-CSE KO HFpEF (n=10)
Log [SNP], M
L
Survival (%)
p < 0.05
Time (weeks)

Figure 5

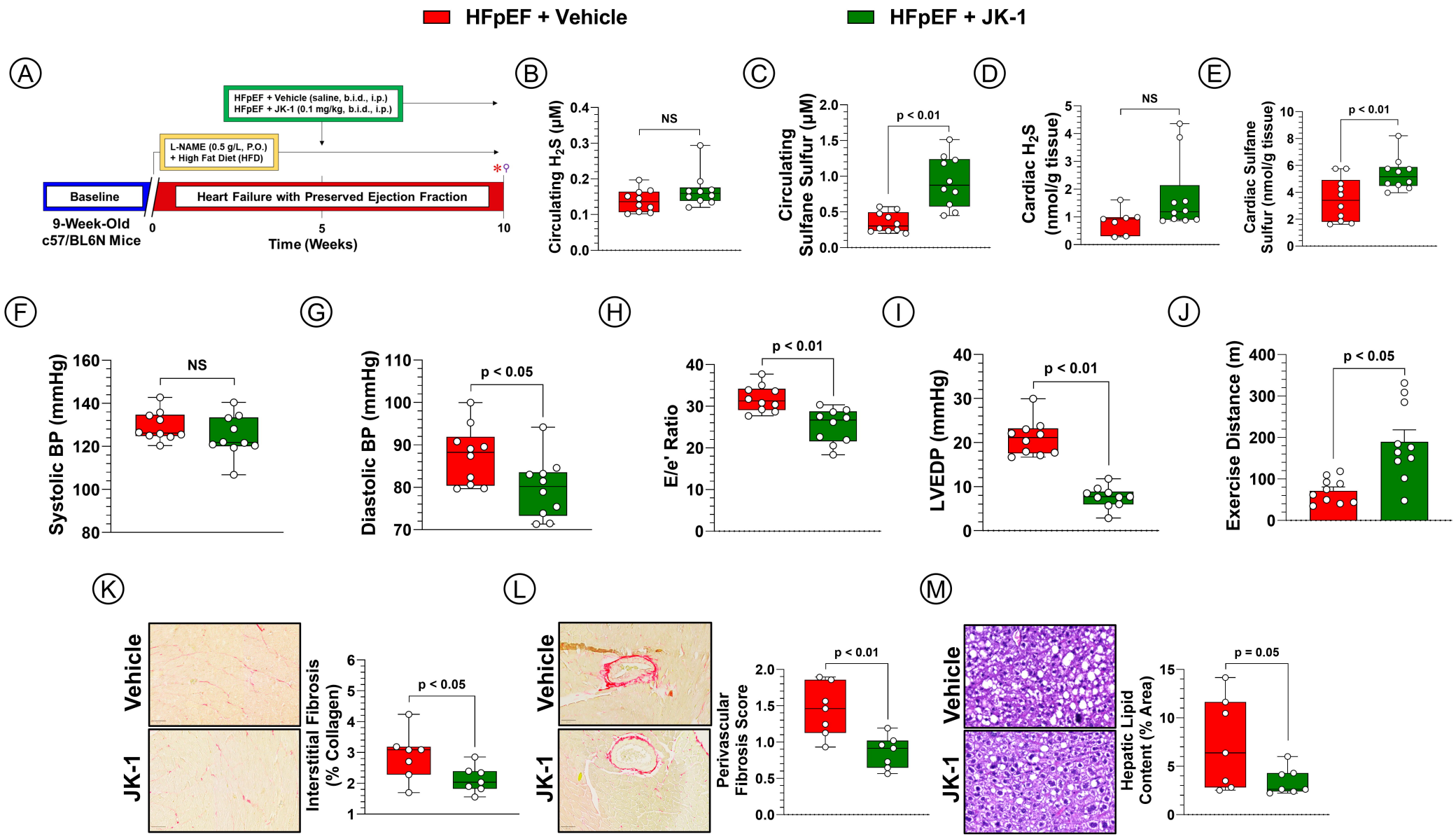
HFpEF + Vehicle
HFpEF + JK-1
A
HFpEF + Vehicle (saline, b.i.d., i.p.)
HFpEF + JK-1 (0.1 mg/kg, b.i.d., i.p.)
L-NAME (0.5 g/L, P.O.)
+ High Fat Diet (HFD)
Baseline
Heart Failure with Preserved Ejection Fraction
9-Week-Old
c57/BL6N Mice
0
5
10
Time (Weeks)
B
Circulating H2S (μM)
NS
C
Circulating Sulfane Sulfur (μM)
p < 0.01
D
Cardiac H2S (nmol/g tissue)
NS
E
Cardiac Sulfane Sulfur (nmol/g tissue)
p < 0.01
F
Systolic BP (mmHg)
NS
G
Diastolic BP (mmHg)
p < 0.05
H
E/e' Ratio
p < 0.01
I
LVEDP (mmHg)
p < 0.01
J
Exercise Distance (m)
p < 0.05
K
Vehicle
JK-1
Interstitial Fibrosis (% Collagen)
p < 0.05
L
Vehicle
JK-1
Perivascular Fibrosis Score
p < 0.01
M
Vehicle
JK-1
Hepatic Lipid Content (% Area)
p = 0.05

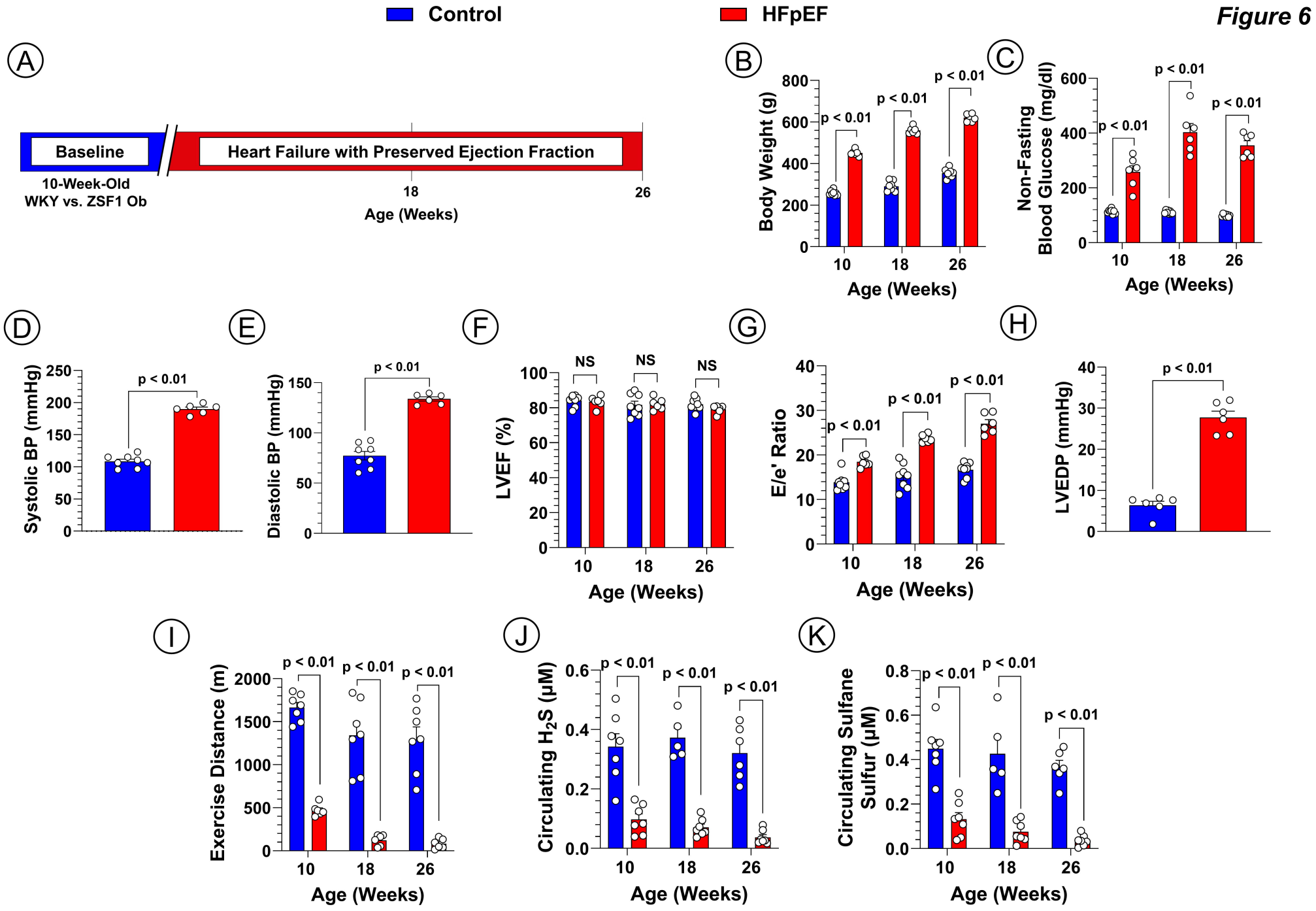
Control
HFpEF
Figure 6
A
Baseline
Heart Failure with Preserved Ejection Fraction
10-Week-Old
WKY vs. ZSF1 Ob
18
26
Age (Weeks)
B
Body Weight (g)
p < 0.01
Age (Weeks)
C
Non-Fasting Blood Glucose (mg/dl)
p < 0.01
Age (Weeks)
D
Systolic BP (mmHg)
p < 0.01
E
Diastolic BP (mmHg)
p < 0.01
F
LVEF (%)
NS
Age (Weeks)
G
E/e' Ratio
p < 0.01
Age (Weeks)
H
LVEDP (mmHg)
p < 0.01
I
Exercise Distance (m)
p < 0.01
Age (Weeks)
J
Circulating H_2S (μM)
p < 0.01
Age (Weeks)
K
Circulating Sulfane Sulfur (μM)
p < 0.01
Age (Weeks)

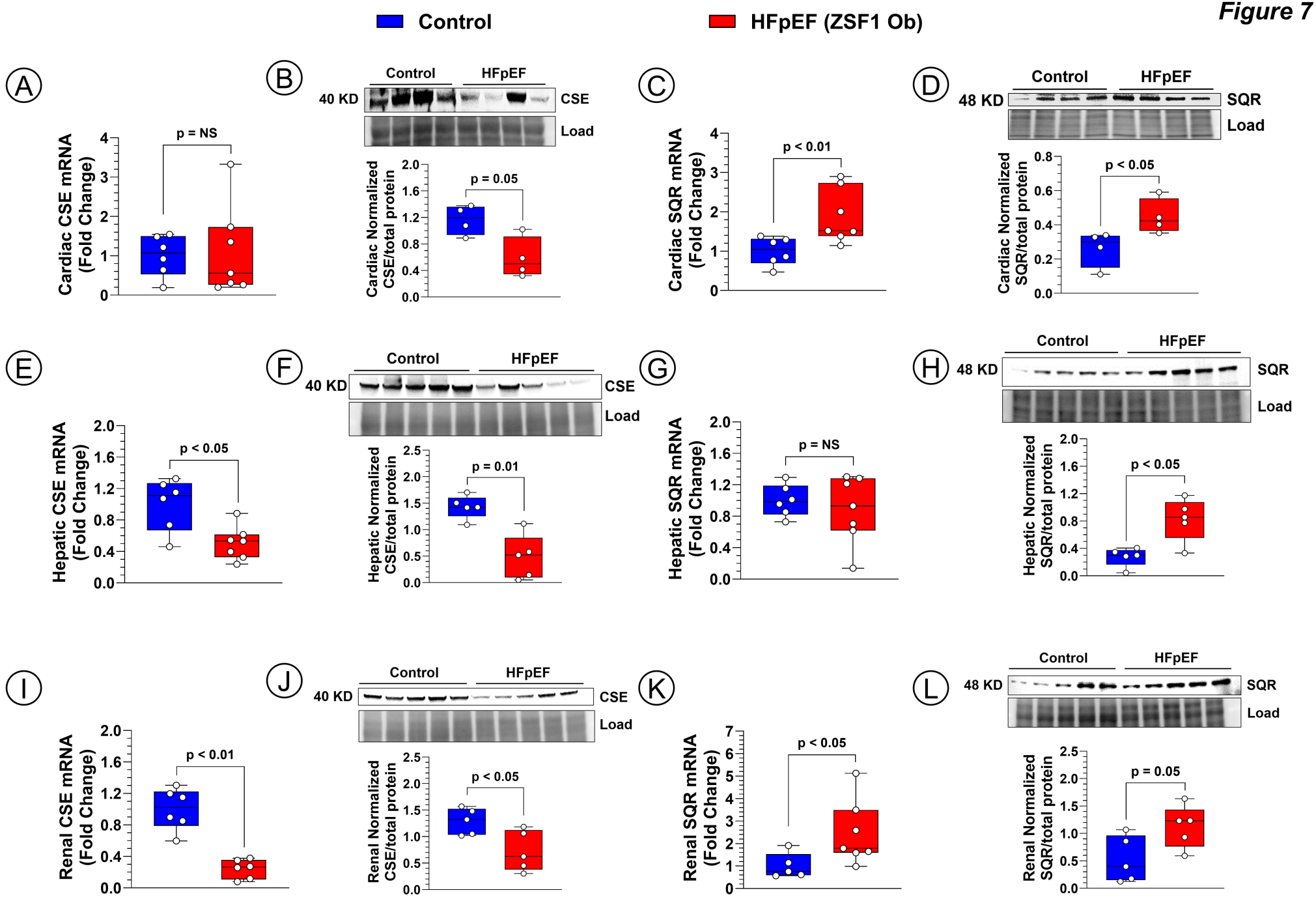
Figure 7
Control
HFpEF (ZSF1 Ob)
A
Cardiac CSE mRNA (Fold Change)
p = NS
B
Control
HFpEF
40 KD
CSE
Load
Cardiac Normalized CSE/total protein
p = 0.05
C
Cardiac SQR mRNA (Fold Change)
p < 0.01
D
Control
HFpEF
48 KD
SQR
Load
Cardiac Normalized SQR/total protein
p < 0.05
E
Hepatic CSE mRNA (Fold Change)
p < 0.05
F
Control
HFpEF
40 KD
CSE
Load
Hepatic Normalized CSE/total protein
p = 0.01
G
Hepatic SQR mRNA (Fold Change)
p = NS
H
Control
HFpEF
48 KD
SQR
Load
Hepatic Normalized SQR/total protein
p < 0.05
I
Renal CSE mRNA (Fold Change)
p < 0.01
J
Control
HFpEF
40 KD
CSE
Load
Renal Normalized CSE/total protein
p < 0.05
K
Renal SQR mRNA (Fold Change)
p < 0.05
L
Control
HFpEF
48 KD
SQR
Load
Renal Normalized SQR/total protein
p = 0.05

Figure 8

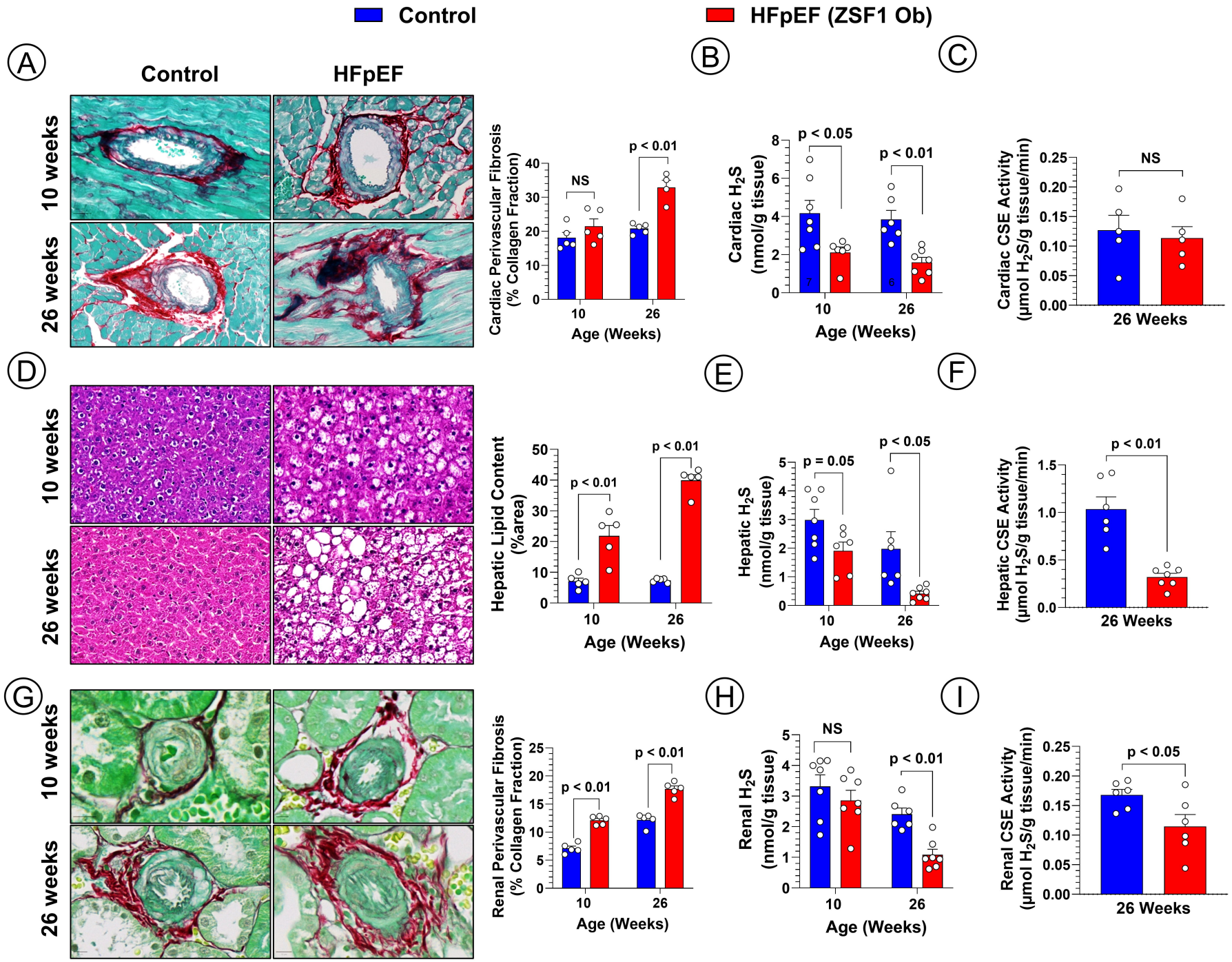
Control
HFpEF (ZSF1 Ob)
A
Control
HFpEF
10 weeks
26 weeks
B
Cardiac Perivascular Fibrosis (% Collagen Fraction)
NS
p < 0.01
Age (Weeks)
C
Cardiac H2S (nmol/g tissue)
p < 0.05
p < 0.01
Age (Weeks)
Cardiac CSE Activity (µmol H2S/g tissue/min)
NS
26 Weeks
D
E
Hepatic Lipid Content (%area)
p < 0.01
p < 0.01
Age (Weeks)
F
Hepatic H2S (nmol/g tissue)
p = 0.05
p < 0.05
Age (Weeks)
Hepatic CSE Activity (µmol H2S/g tissue/min)
p < 0.01
26 Weeks
G
H
Renal Perivascular Fibrosis (% Collagen Fraction)
p < 0.01
p < 0.01
Age (Weeks)
I
Renal H2S (nmol/g tissue)
NS
p < 0.01
Age (Weeks)
Renal CSE Activity (µmol H2S/g tissue/min)
p < 0.05
26 Weeks